

**ELECTROCHEMICAL PREPARATION AND INVESTIGATION  
OF PHOTOELECTROCATALYTIC PROPERTIES OF ZnO  
FILMS DECORATED WITH Cu<sub>2</sub>O NANOCUBES**

**Ako Mahmood QADIR**

**Master Thesis**

**Department of Chemistry**

**Advisor: Prof. Dr. İbrahim Y. ERDOĞAN**

**January 2017**

**All rights reserved**

**REPUBLIC OF TURKEY  
BİNGÖL UNIVERSITY  
INSTITUTE OF SCIENCE**

**ELECTROCHEMICAL PREPARATION AND  
INVESTIGATION OF  
PHOTOELECTROCATALYTIC PROPERTIES OF  
ZnO FILMS DECORATED WITH Cu<sub>2</sub>O  
NANOCUBES**

**MASTER THESIS**

**Ako Mahmood QADIR**

**Department Institute : Chemistry (Analytical Chemistry)**

**Advisor of Thesis : Prof. Dr. İbrahim Y. ERDOĞAN**

**January 2017**

REPUBLIC OF TURKEY  
BİNGÖL UNIVERSITY  
INSTITUTE OF SCIENCE

**ELECTROCHEMICAL PREPARATION AND INVESTIGATION  
OF PHOTOELECTROCATALYTIC PROPERTIES OF ZnO  
FILMS DECORATED WITH Cu<sub>2</sub>O NANOCUBES**

**MASTER'S THESIS**

**Ako Mahmood QADIR**

**Department : CHEMISTRY**

**This dissertation was accepted by the following committee on 20.01.2017 with the vote unity.**

**Assoc. Prof. Dr.  
Ramazan SOLMAZ  
Head of examining  
committee**

**Asst. Prof. Dr.  
Feride AKMAN  
Member of examining  
committee**

**Prof. Dr.  
İbrahim Y. ERDOĞAN  
Member of examining  
committee**

**I confirm the result above**

**Prof. Dr. İbrahim Y. ERDOĞAN  
Director of the institute**

## **PREFACE**

First of all, I would like to thank my Lord and my God (Allah), for providing this opportunity of starting and completing my master degree thesis, healthy and successfully.

I also have thanks and respect for a very valuable teacher who has not hesitated in helping me during my thesis work and has provided a stimulating environment for our work. I thank him for his great support. Love and peace to Prof. Dr. İbrahim Yasin ERDOĞAN from the Chemistry department.

I also want to thank my best friend and my supporter to everything in my master degree. Mr Aryan Mahmood Faraj for helping me to finish my MSc.

And then, I thank and respect my parents and my family who have always given their financial and spiritual support. In addition, I have special thanks to the best student of (MSc), who has helped me in my laboratory practical work, Mrs Meral Balık.

Finally, I would like to thank my wife for her support and help in completing this thesis. Best wishes for my wife and my crazy baby!

**AkoMahmood QADIR**

**Bingöl 2017**

# CONTENTS

PREFACE .....	ii
CONTENTS .....	iii
LIST OF SYMBOLS AND ABBREVIATIONS .....	v
LIST OF FIGURES .....	vii
ÖZET .....	x
ABSTRACT .....	xi
1. INTRODUCTION .....	1
2. LITERATURE REVIEW .....	15
3. MATERIALS AND METHODS .....	27
3.1. Materials Used in Laboratory Studies .....	27
3.1.1. Chemicals Used .....	27
3.1.2. Instruments and Devices Used in Our Work .....	27
3.1.3. Materials Used in Electrochemical Studies .....	27
3.1.3.a. Properties and specializing of Solvent and Electrolyte..	28
3.1.3.b. The Solutions .....	28
3.1.3.c. Electrochemical Cell .....	29
3.1.3.d. Electrodes .....	29
3.1.3.e. Potentiostat .....	33
3.2. Methods Used .....	34
3.2.1. Electrochemical Methods .....	34
3.2.2. UV-GB Spectroscopy .....	37
3.2.3. SEM .....	38
3.2.4. EDX .....	40
3.2.5. XRD .....	41

3.2.6. PhotoelectrochemicalSystem .....	44
4. FINDINGS AND DISCUSSION .....	45
4.1. Electrochemical Studies .....	45
4.2. XRD Studies .....	46
4.3. SEM and EDX Studies .....	49
4.4. Absorbance and band Gap Studies .....	53
4.5. PEC Studies .....	57
5. RESULTS AND RECOMMENDATIONS .....	61
REFERENCES .....	64
CURRICULUM VISIT .....	72

## LIST OF SYMBOLS AND ABBREVIATIONS

CBD	: chemical bath deposition
CBM	: conduction band minimum
cm <sup>2</sup>	: Centimeters meter square
CV	: Cyclic voltammetry
CVD	: Chemical Vapor Deposition
d	: distance
E	: electron potential
E <sup>0</sup>	: Standard electrode potential
ED	: Electrodeposition
E <sub>g</sub>	: energy band
ev	: Electron volts
FETs	: field-effect transistors g:Gram
I <sub>pa</sub>	: Anodic peak current
I <sub>pc</sub>	: Cathodic peak current
K	: Kelvin
Kj	: Kilojoule
L	: litter
Log	: Logarithmm
mV	: Milivolt
n	: Number of electrons
nm	: Nanometer
Pa	: Pascal
s	: second
Scm	: Standard cubic centimeter-minute
T	: temperature

t : time  
UPD : underpotential depth  
V : Volt  
 $\Omega$  : Electrical resistance  
 $\lambda$  : Wavelength



## LIST OF FIGURES

Figure 1.1.	The working principle of solar cells .....	6
Figure 1.2.	The triangle pathways between mechanical, electrical, and thermal piezoelectric effect, pyroelectric effect .....	9
Figure 1.3.	Schematically representation crystal structures of ZnO: (a) Rochelle salt or cubic rocksalt, (b) cubic zinc blende, (c) hexagonal wurtzite , gray spheres denote Zn atoms, and black spheres denote O atoms .....	10
Figure 3.1.	The pure water system that use for ultra-pure water .....	28
Figure 3.2.	Electrochemical cell display .....	29
Figure 3.3.	Saturated calomel electrode .....	30
Figure 3.4.	Change of electrode potential with temperature .....	31
Figure 3.5.	Ag / AgCl reference electrode .....	31
Figure 3.6.	Platinum counter electrodes .....	32
Figure 3.7.	Schematic representation of the potentiostatic components used in electrochemical studies .....	33
Figure 3.8.	Schematic representation of the potentiostat system used in our studies ..	34
Figure 3.9.	Cyclic voltammetric technique for conversion the potential vs time .....	35
Figure 3.10.	Schematically representation of Double beam spectrometer .....	37
Figure 3.11.	Shimadzu UV-3600 UV-VIS-NIR Spectrophotometer used in our work ..	38
Figure 3.12.	Schematically representation the main components of SEM are electron column scanning system .....	39
Figure 3.13.	The EDX and SEM system in our studies (JEOL JSM-6510) .....	41
Figure 3.14.	Schematic diagram of Bragg's reflection from lattice planes in a crystalline structure by development of x-ray diffraction.....	42
Figure 3.15.	The XRD device (Rigaku Ultima IV) .....	43
Figure 3.16.	Schematic representation of the instrument in photoelectrochemical measurements .....	44

Figure 4.1.	The XRD diffractogram of ZnO electrodeposited onto ITO coated coated glass surface.....	46
Figure 4.2.	The XRD diffractogram of ZnO films decorated with Cu <sub>2</sub> O nanocubes electrodeposited for 1 min .....	47
Figure 4.3.	The XRD diffractogram of ZnO films decorated with Cu <sub>2</sub> O nanocubes electrodeposited for 3 min .....	47
Figure 4.4.	The XRD diffractogram of ZnO films decorated with Cu <sub>2</sub> O nanocubes electrodeposited for 5 min .....	48
Figure 4.5.	The XRD diffractogram of ZnO films decorated with Cu <sub>2</sub> O nanocubes electrodeposited for 10 min .....	48
Figure 4.6.	The XRD diffractogram of ZnO films decorated with Cu <sub>2</sub> O nanocubes electrodeposited for 15 min .....	49
Figure 4.7.	SEM image of ITO coated glass surface .....	50
Figure 4.8.	SEM image of ZnO films electrodeposited onto ITO coated glass..	50
Figure 4.9.	SEM image of ZnO films decorated with Cu <sub>2</sub> O nanocubes electrodeposited for 1 min .....	51
Figure 4.10.	SEM image of ZnO films decorated with Cu <sub>2</sub> O nanocubes electrodeposited for 3 min .....	51
Figure 4.11.	SEM image of ZnO films decorated with Cu <sub>2</sub> O nanocubes electrodeposited for 5 min .....	52
Figure 4.12.	SEM image of ZnO films decorated with Cu <sub>2</sub> O nanocubes electrodeposited for 10 min .....	52
Figure 4.13.	SEM image of ZnO films decorated with Cu <sub>2</sub> O nanocubes electrodeposited for 15 min .....	53
Figure 4.14.	Absorbance spectrum of ZnO films electrodeposited onto ITO coated glass surface .....	54
Figure 4.15.	Absorbance spectrum of ZnO films decorated with Cu <sub>2</sub> O nanocubes electrodeposited for 1 min .....	54
Figure 4.16.	Absorbance spectrum of ZnO films decorated with Cu <sub>2</sub> O nanocubes electrodeposited for 3 min .....	55
Figure 4.17.	Absorbance spectrum of ZnO films decorated with Cu <sub>2</sub> O nanocubes electrodeposited for 5 min .....	55

Figure 4.18.	Absorbance spectrum of ZnO films decorated with Cu <sub>2</sub> O nanocubes electrodeposited for 10 min .....	56
Figure 4.19.	Absorbance spectrum of ZnO films decorated with Cu <sub>2</sub> O nanocubes electrodeposited for 15 min .....	56
Figure 4.20.	Linear sweep voltammograms of ZnO films electrodeposited onto ITO coated glass surface in 0.1 M Na <sub>2</sub> SO <sub>4</sub> .....	57
Figure 4.21.	Linear sweep voltammograms of ZnO films decorated with Cu <sub>2</sub> O nanocubes electrodeposited for 1 min in 0.1 M Na <sub>2</sub> SO <sub>4</sub> .....	58
Figure 4.22.	Linear sweep voltammograms of ZnO films decorated with Cu <sub>2</sub> O nanocubes electrodeposited for 3 min in 0.1 M Na <sub>2</sub> SO <sub>4</sub> .....	58
Figure 4.23.	Linear sweep voltammograms of ZnO films decorated with Cu <sub>2</sub> O nanocubes electrodeposited for 5 min in 0.1 M Na <sub>2</sub> SO <sub>4</sub> .....	59
Figure 4.24.	Linear sweep voltammograms of ZnO films decorated with Cu <sub>2</sub> O nanocubes electrodeposited for 10 min in 0.1 M Na <sub>2</sub> SO <sub>4</sub> .....	59
Figure 4.25.	Linear sweep voltammograms of ZnO films decorated with Cu <sub>2</sub> O nanocubes electrodeposited for 15 min in 0.1 M Na <sub>2</sub> SO <sub>4</sub> .....	60
Figure 4.26.	Photocurrent responses of the films under light illumination in 0.1 M Na <sub>2</sub> SO <sub>4</sub> . Black line show photocurrent density of ZnO films electrodeposited onto ITO coated glass. Current density of ZnO films decorated with different Cu <sub>2</sub> O nanocubes (brown line, 1 min; red line, 3 min orange line, 5 min; blue line, 10 min; gray line, 15 min.....	60

# **Cu<sub>2</sub>O NANOKÜPLERİ İLE DONATILMIŞ ZnO FİMLERİNİN ELEKTROKİMYASAL YÖNTEMLE HAZIRLANMASI ve FOTOELEKTROKATALİTİK ÖZELLİKLERİNİN İNCELENMESİ**

## **ÖZET**

Bu tez çalışması, ZnO filmlerinin yapısal, optik ve fotoelektrokimyasal özelliklerine Cu<sub>2</sub>O nanoküplerinin katılmasının etkisi üzerine sistematik bir çalışmadır. Cu<sub>2</sub>O nanoküpleri ile donatılan ZnO filmleri potansiyelaltı depozisyon (UPD) temelli pratik bir elektrokimyasal yöntem kullanılarak hazırlandı. Cu<sub>2</sub>O nanoküpleri ile donatılan ZnO filmlerinin detaylı karakterizasyonu X-ışını kırınımı (XRD), taramalı elektron mikroskopu (SEM), enerji dağılımlı X-ışını spektroskopisi (EDX), morötesi-görünür bölge (UV-Vis) spektroskopisi ve fotoelektrokimyasal (PEC) teknikler kullanılarak gerçekleştirildi. XRD ve UV-Vis spektroskopi sonuçları; 5 dakika depozisyon zamanı için ikinci bir faz olan Cu<sub>2</sub>O'ın ortaya çıktığını, daha düşük depozisyon zamanları için ( $\leq 3$  dakika) tek faz ZnO oluştuğunu gösterdi. Absorbans spektrumlarından belirlenen optiksel bant aralığı enerjisi ve EDX sonuçları ZnO ve Cu<sub>2</sub>O varlığını doğrular. SEM görüntüleri, ZnO üzerine depozit edilen küp-biçimli Cu<sub>2</sub>O nanokristallere sahip bir morfoloji gösterdi. Bu çalışma, 3 dakika büyütülen Cu<sub>2</sub>O nanoküpleri ile katılan ZnO filmlerinin en iyi PEC performansına sahip olduğunu gösterdi. Cu<sub>2</sub>O nanoküpleri ile dekore edilen ZnO filmleri, ileri PEC dedeksiyonu, PEC su ayrıştırma ve diğer solar fotovoltaik teknolojilerinin geniş bir alanı için rekabetçi bir aday olarak önerilir.

**Anahtar Kelimeler:** ZnO, Cu<sub>2</sub>O, elektrodepozisyon, ve fotoelektrokimya.

# **ELECTROCHEMICAL PREPARATION AND INVESTIGATION OF PHOTOELECTROCATALYTIC PROPERTIES OF ZnO FILMS DECORATED WITH Cu<sub>2</sub>O NANOCUBES**

## **ABSTRACT**

This thesis work reports on a systematic study of the influence of Cu<sub>2</sub>O nanocubes doping on the structural, optical and photoelectrochemical characteristics of ZnO films. ZnO films decorated with Cu<sub>2</sub>O nanocubes were prepared by practical electrochemical method, based on the underpotential deposition (UPD). A detailed characterization of ZnO films decorated with Cu<sub>2</sub>O nanocubes was performed by X-ray diffraction (XRD), scanning electron microscopy (SEM), energy dispersive X-ray spectroscopy (EDX), ultraviolet–visible (UV–Vis) spectroscopy and photoelectrochemical (PEC) techniques. The XRD and UV–Vis spectroscopy results showed single phase ZnO for the lower Cu<sub>2</sub>O deposition time (at time ≤ 3 min), while a secondary phase of Cu<sub>2</sub>O evolved for 5 min deposition time. The optical band gap, determined from the absorbance spectra, and EDX results confirm the presence of ZnO and Cu<sub>2</sub>O. SEM images show morphology with cube-shaped Cu<sub>2</sub>O nanocrystals deposited over ZnO film. This work showed that ZnO films doped with Cu<sub>2</sub>O nanocubes grown for 3 min have the best PEC performance. ZnO films decorated with Cu<sub>2</sub>O nanocubes are suggested as a competitive candidate for advanced PEC detection, maybe for the extended field of PEC water splitting and other solar photovoltaic technologies.

**Keywords:** ZnO, Cu<sub>2</sub>O, electrodeposition, and photoelectrochemistry.

## 1. INTRODUCTION

Semiconductor materials are widely used for diode, transistor, rectifier, capacitor, thermistor, computer, hard disk, USB flash drive, graphics processors radar, satellite communications, solar panels. Semiconducting nanotechnology with controlling size, structure, and orientation playing an important role in the fabrication and various applications such as photovoltaic cells (PVs), field-effect transistors (FETs), thermoelectric (TE) devices, memory elements, photodetectors (PDs), diodes, light emitting diodes (LEDs), nanolasers, chemical and biological sensors (Reut et al. 2016). In addition, various techniques and methods have been used for preparation of semiconductormetals, such as deposition, using high-energy sources, deposition precipitation, and ultrahigh vacuum sputter coating, these techniques are used to produce nanoparticles with wide size distribution and non-uniform clusters. To overcome the difficulty of weak interactions between metal oxide and metal, various works have been made to modify and provide the better surface of metal oxide with an intermediate layer such as polymers, surfactants, or amorphous Si-OH polymers. These modifications provide new functional groups such as thiols, amines and carboxylates, which introduce covalent linkages between metal oxide and metals (Pan et al. 2012).

Some commonly used semiconductors and semiconducting materials and areas of use:

- ✓ Copper (I) oxide ( $\text{Cu}_2\text{O}$ ): Diode in solar applications
- ✓ Copper (II) oxide ( $\text{CuO}$ ): The sensor is in the solar battery
- ✓ Boron (B), Indium (In), Gallium (Ga): To form a p-type semiconductor
- ✓ Silicon (Si) and Germanium (Ge): In making diode, transistor, integrate
- ✓ Antimon (Sb), Phosphorus (P), Arsenic (Ar): To make n-type semiconductor.

An important branch of nanotechnology contains the fabrication of nanostructure based gas sensors with high selectivity, sensitivity, stability, recovery time and improved response. These techniques are commonly used for synthesizing nanomaterials, and also

they were provided a powerful control for the physical properties of the products, such as shape, size, and composition. In most cases, metal oxides, which have a transducer function and receptor, are used as gas-sensing materials as their resistances of electrical will change correspondingly upon exposure to reducing gases or oxidizing gases. In the sensing process, specific interaction between target molecules and a metal oxide surface is required and also the materials should be in large ability to transfer the interaction induced alterations from the surfaces into a macroscopically accessible signal, typically, a change in the electrical resistance (Liu et al. 2012).

Various oxide semiconductor based gas sensors have been used to detect harmful and toxic gases. The most sensor materials such as SnO<sub>2</sub>, ZnO, In<sub>2</sub>O<sub>3</sub>, Fe<sub>2</sub>O, Co<sub>3</sub>O<sub>4</sub>, TiO<sub>2</sub>, WO<sub>3</sub> show excellent gas-sensing properties to oxidizing or reducing gases has been studied and applying in many fields such as ultraviolet detection, solar cell, sensor and luminescence. Zinc oxide nanomaterial has an excellent gas-sensing material with high sensitivity to ppm level and sometimes even better. In addition, an important factor for the stability of the sensor is a microstructure stability which has less agglomeration and better morphology maintenance, On the other hand, noble metals, explained as active catalysts, have been enhanced the promoting effects on many semiconductor gas sensors (Lin et al. 2015).

Except inorganic semiconductors, organic semiconductor nanoparticles (OSNs), with some special characterization include  $\pi$ -conjugate structures, good optical properties and electronic properties. They used a wide range of applications in biochemical sensors and optoelectronic devices (Anthony et al. 2010). In addition, preparation of metal nanoparticles, luminescent nanoparticles, magnetic nanoparticles, spray route, spray pyrolysis, salt assisted spray pyrolysis (SASP), chemical vapor deposition (CVD) and agglomeration particle control (Okuyama et al. 2005).

Zinc is an important transition metal element and Zn<sup>2+</sup> has close ionic radius parameter to that of Cu<sup>2+</sup>, which means that Zn can easily penetrate into CuO crystal lattice or substitute Cu position in the crystal. Thus, ZnO/Cu<sub>2</sub>O thin film solar cells are prepared by electrodeposition.

Electrodeposition is a technique low temperature process of energy used to make those materials which are used in computer chips and magnetic data storage systems with lower the cost and improve the performance of our information society. In addition, also used for producing those structures that used in a nanotechnology, nano biotechnology based future (Bartlett et al. 2004).

Transparent conductive oxide film has high permeability in the visible region and is obtained from semiconductor materials with low electrical resistivity. Transparent conductive oxides such as ZnO, SnO<sub>2</sub>, In<sub>2</sub>O<sub>3</sub> and ITO as n-type materials are used in many optoelectronic systems have large applications. Cu<sub>2</sub>O is material transparent conductive oxides with p-type conductivity, and by joining p-type and n-type, p-n obtain which very important materials for devices (Alkoy and Kelly 2005).

Photoelectrochemical measurement is potentially a sensitive as electrochemiluminescence (ECL) owing to the complete separation of excitation light source and detection photocurrent signal, it is newly developed and promising analytical technique the utilization of electronic detection makes the photo electrochemical instruments simpler and low cost. The sensitive photo electrochemical determination based on excellent photoelectric light with the enhanced response of photo and promoted photoelectric conversion efficiency. Most of the designs are rely on heterojunction of semiconductor, and surface Plasmon resonance of noble metal, among the above methods, the properties of the semiconductor heterojunction dominate the behavior of photo induced charge carriers, such as the transport direction, the separation distance, and the recombination rate (Li et al. 2014).

Photocatalytic efficiency of a semiconductor material have attracted considerable attention for both energy application and environment fields, it depends on the photogenerated electron hole separation processes. Therefore, forming metal/semiconductor heterostructures can reduce the rate of recombination electron-hole, thereby increasing the efficiency of photocatalytic the formation of heterostructures between the semiconductors with varied majority carrier type is an alternative effort to increase the hole of electron lifetime, by forming junction between n-type and p-type semiconductors a depletion layer at the region of p-n interfacial can be produced that



induces an electric field. Some important major factors have been studied in controlling photocatalytic efficiencies and their optical properties, which highly depends on size, impurities, dopants, and morphology of the materials, On the other hand, the optoelectronic properties, and the performance catalytic of semiconductor materials also depend on the surface area and also the number of active sites present on the catalyst surface. Thus, controlling of morphology and size of the photocatalyst require to get efficient, active sites and reproducible photocatalytic properties. The nanoparticles have been exhibited uniform size and morphology especially desirable in production of semiconductor material, as the synthesis of uniform surface area, morphology, and active sites photocatalytic properties (Kandjani et al. 2015).

The major problems that hinder the development of society is the environmental pollution and energy crisis, the researchers believed that in order to solve these crisis of fossil fuel depletion, they used photocatalytic decomposition of water, which uses solar energy to split water, providing clean hydrogen energy, while the photocatalytic degradation of toxic organic pollutants is thought to be an inexpensive and feasible way of addressing environmental issues (Zhu et al. 2010). on the other side. Fossil fuels are the major part of energy sources consumed on the world today. However, their combustion products are causing the global problems, such as the greenhouse effect, ozone layer depletion, acid rains, and pollution, which are posing a great danger for our environment and eventually for the life in our planet, therefore, the scientists and the researchers were tried to find an alternative energy sources to maintain the current life standards. Many scientists agree that replace to the hydrogen energy system. Hydrogen is a secondary form of energy or an energy carrier. Although there are some production methods, hydrogen gas can be produced in large quantities by water electrolysis. The electricity needed for the electrolysis can be supplied by renewable energy sources such as solar cells (Solmaz et al. 2016).

Renewable energy sources have been a research field that has been researched frequently in order to meet the rising energy demand in our country and the world also has been carrying out serial production. When someone thinks of renewable energy, should be thinking of costs, clean, cheap and long lasting power unit. Such as life source water is an inexhaustible natural resource and hydrogen is a renewable, sustainable and clean energy

source, the breakdown of hydrogen and oxygen water with minimal fuel consumption is one of the most important chemical processes related to energy. Solar energy is an important renewable energy source, considered as a major alternative to existing energy and environmental problems.

Solar cell power is also considered one of the cleanest of renewable energy resources, the public opinion, too, is particularly favorable to the use of solar energy, which seems to be without any environmental impact. A typical solar cell exists of n-type emitter, p-type emitter, front- and back electrodes and an antireflective coating. The active n-type and p-type make up the p-n junction where generate electricity, to increase the total output Solar cells strings are connected in series. also to protect effective of the solar cells from stress of mechanical, weathering and humidity, by stringing the cell in a transparent bonding material that applied to a substrate; usually glass, but acrylic plastic, metal or plastic sheeting can also be used. It is common that excitons occurs in the active layer of organic solar cells, it have a distance of excitons migration are much small less than 20 nm, therefore, the distance for migration and diffusion to the interface of electron acceptors and electron donors in organic solar cells, it should be less than 20 nm to obtain best efficient of light conversion(Stoppato 2008).

Solar cells are photovoltaic (PV) cells that generate electrical energy by converting absorbed sunlight coming to the surface directly into direct current (DC) electrical energy, then through converters change to suitable AC grid electricity. Photovoltaic modules have ability between 5 to 20 % depending on their types. Some parameters such as internal resistance, contact structure, the material used, a variation of temperature and light density are affected by the efficiency of solar cells. Most of the electrons are included in n-type semiconductor material while most of the electrons hole included in p-type semiconductor material. Sun light breaks electron from the n-type semiconductor material. Energizing electrons flow of p-type to the n-type semiconductor material via an external circuit by movement and flow of electrons forms direct current (DC). Electrons flowing through the founded circuit which is used for the charging of batteries or different fields return to the p-type semiconductor material. In this way, electrical energy is obtained from solar cells (Şahin and Okumuş 2016).

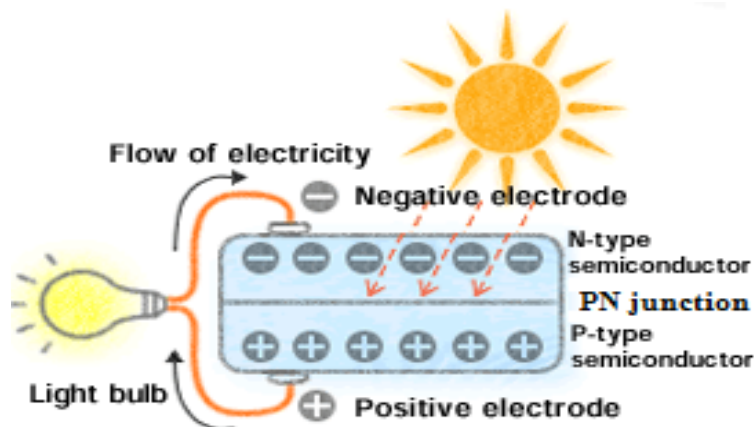


Figure 1.1. The working principle of solar cells(Şahin and Okumuş 2016)

Solar cells are manufactured from ingots. It can be in mono or polycrystalline form. A mono crystal ingot is obtained by pulling the crystal from the silicon melt. The process is named after Polish scientist Jan (Czochralski 1918) who invented the method while investigating the crystallization rates of metals. The polycrystalline ingot is melted in a vessel and is obtained by repeated freezing in another vessel (Bridgeman 1925), the method and the silicon casting are the most common methods for manufacturing multi-crystalline ingots. Zinc oxide absorbs only about 5% of sunlight, it has wide band gap semiconductor, must be the band gap of zinc oxide to be narrowed to absorb visible light, which can be achieved by doping some transition metal ions, e.g., Mn, Ni, Co, Ag, Cd, Cu. Researchers have performed doping in metal oxides for getting better optical, electrical properties and crystallization quality. Cu oxide is one of the most important compound semiconductors with many applications, such as magnetic storage media, field transistors, photovoltaic applications, superconductors, methanol synthesis and gas sensors (Sáenz et al. 2014).

Photoelectrochemical cells are solar cells that convert light source to electrical energy, by this process generate electrical energy including the visible region. Each cell consists of a photocathode and a metal anodant put in an electrolyte. Semiconductor technology is the basis of solar cell systems, which is a very important place for energy production. A photoelectrochemical process takes three steps. In the first step, an electronic charge is formed on the surface of the photocathode sensitive to the sun's rays, forming electron-hole pairs. In the second step, electrons and protons in the photocathode are reduced to

hydrogen molecules. In the third step, the conduction of the photocathotically anodic holes is via electrolytic and electrical connection, respectively. the process of absorption as common standard processes in semiconductors happen from crystalline material, thin epitaxial, amorphous films, polycrystalline or quantum dots, in clusters, dyes and macromolecules or in nanocomposite materials ( Sze et al. 2007).

Semiconductor photocatalysts have attracted considerable attention for both fundamental research and practical application in energy and environment fields. Especially,  $\text{Cu}_2\text{O}$  is of great importance exhibit some unique chemical and physical properties such as narrow band gap, reasonable cost, low toxicity, good environmental acceptability, and strong adsorption of molecular oxygen. These advantages have contributed to the application of  $\text{Cu}_2\text{O}$  in the visible light photocatalytic degradation of organic pollutants. It is well-known that the performances of a single phase semiconductor are strongly dependent on its size, shapes, and crystallization (Kim et al. 2012).

Metal oxide nanoparticles (NPs) are attracting considerable attention for their potential applications in different fields, e.g., optoelectronics and nanoelectronics, gas sensing, catalysis, and so on. Among various metal oxides, copper oxide nanoparticles (NPs) are particularly interesting to use in a range of physical properties. Synthesis of semiconductor nanomaterials had become an important role in material science research with controlled size, shape, and crystallographic orientation, e.g., a narrow band gap  $\text{Bi}_2\text{Te}_3$  and other V–VI group semiconductors are described as the favorable materials for thermoelectric (TE) applications at room temperature and they wide applications that can be used for biomedical and optoelectronic applications such as infrared sensors, photo detectors, power generation, heat pumps, solid state refrigeration and optoelectronic sensors (Erdoğan and Demir 2011). Porous metal oxide semiconductors with series of applications such as catalysts, lithium-ion batteries, drug delivery release and chemical sensors, have been an important specific topic in material science due to of their superior performances compared with other solid counterparts. It is evident the porous structure has ability to increase the ratio of surface-to-volume and surface area of materials, thus improving the efficiency of reaction on material surfaces and resulting in enhanced properties or performance. Researchers have indicate that porous semiconductors are promising candidates for catalysts or sensor materials in that the gas diffusion or mass

transport in such materials is much more convenient and effective compared with solid ones. Often the sacrificial templates or structure-directing agents are required to generate pores and cavities in a material matrix or synthesis of porous material. For instance, porous  $\text{Fe}_2\text{O}_3$ ,  $\text{Co}_3\text{O}_4$  and  $\text{ZnO}$  are economically produced by annealing, with using of hydroxide or carbonate as precursor of preparation, non-template synthetic methods for porous materials have been reported (Liu et al. 2010).

Zinc oxide is one of the n-type group II-VI semiconductors, its wide band gap (3.37 eV), it has relatively higher and stable exciton binding energy of 60 meV at room temperature 300 K, its white color solid inorganic powder, wurtzite structure crystalline, non-flammable, insoluble in water, it is used in the vulcanization of rubber, ceramics, paints, animal feed and pharmaceuticals, high charge carrier mobility, large electron mobility at room temperature about  $100\text{-}200\text{ cm}^2/\text{V s}$ , great thermal conductivity. The hole mobility at 300 K is approximately  $5\text{-}50\text{ cm}^2/\text{V s}$ , electron/hole effective mass 0.24/ 0.59  $m_0$ . (Yamazoe, et al. 2003). Direct band energy gap and high exciton binding energy allowed zinc oxide preferable for a several devices, including photodetectors, transparent thin-film transistors, light-emitting diodes and laser diodes that work in the blue and ultraviolet region of the spectrum. Zinc oxide is also added to food products and incorporated in vitamin and mineral supplements, in the case of zinc deficiency it provides zinc to soil with fertilizing, widely used in cosmetic, nutritional additive, pharmaceutical and medical applications (Klingshirn et al. 2010). In addition, suitable for a window layer, low dimensional nonstructural, because of possessing of piezoelectric, catalysis properties and optical properties, special physical, chemical properties and electrical properties therefore used for many applications. It can be synthesized by several methods and it can be produce in different structural morphologies include nanowires nanoflowers, thin film, nanorods, nanocorals, nanotubes, and nanowalls and nanoparticles (Jiang et al. 2015). It is found in many electroacoustic applications such as sound sensors, sonar emitters and detectors, and pressure transducers.

$\text{ZnO}$  nano rods are potentially useful for various nano devices such as light emitting diodes (LEDs), chemical sensors, solar cells, and piezoelectric devices, because of their high aspect ratio and large surface area to volume ratio ensure high efficiency and

sensitivity in these applications. Furthermore, ZnO is bio-safe and biocompatible and may be used for biomedical applications without coating (Amin and Willander 2012).

Among the semiconductors zinc oxide (ZnO) has several properties include piezoelectric and pyroelectric, and electrical properties. The well-known triangle pathways described as shown in Figure 1.2, between mechanical, electrical, and thermal energies in a class of those materials exhibiting piezoelectric effect, pyroelectric effect means electro caloric conversion effect, effect of piezocaloric it means thermal expansion conversing.

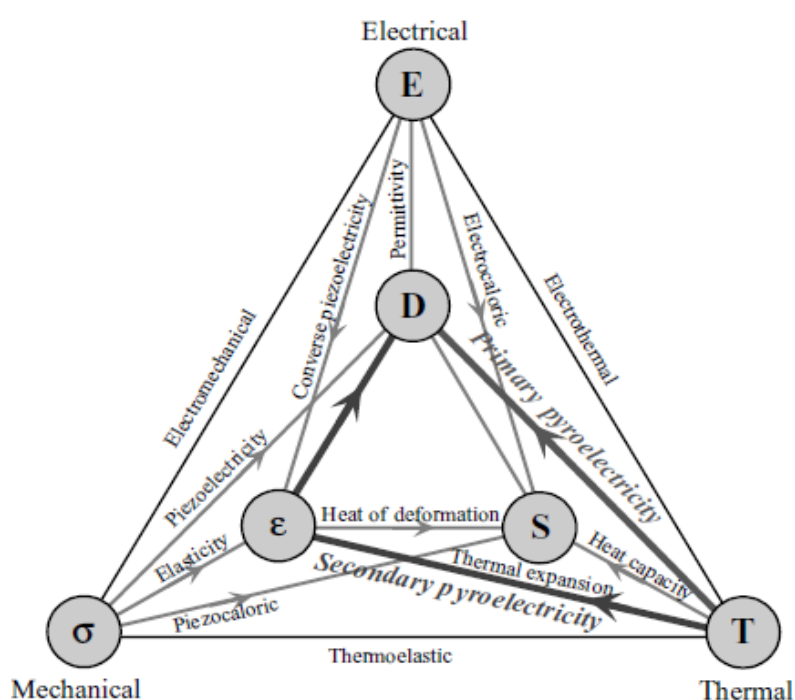


Figure 1.2. The triangle pathways between mechanical, electrical, and thermal, piezoelectric effect, pyroelectric effect (Morkoç et al. 2009)

It is explained that the pyroelectricity of primary contribution is generally more than the secondary effect. In weakly ferroelectric or non-ferroelectric materials such as zinc oxide, the coefficients of pyroelectric are small and relate with the specific heat, due to thermal motions, because all pyroelectric materials are also piezoelectric (Morkoç et al. 2009).

Zinc oxide is one of the semiconductors that have three crystal structures are hexagonal wurtzite, cubic zinc blende, and also cubic rock salt or Rochelle salt, as represented in Figure 1.3.

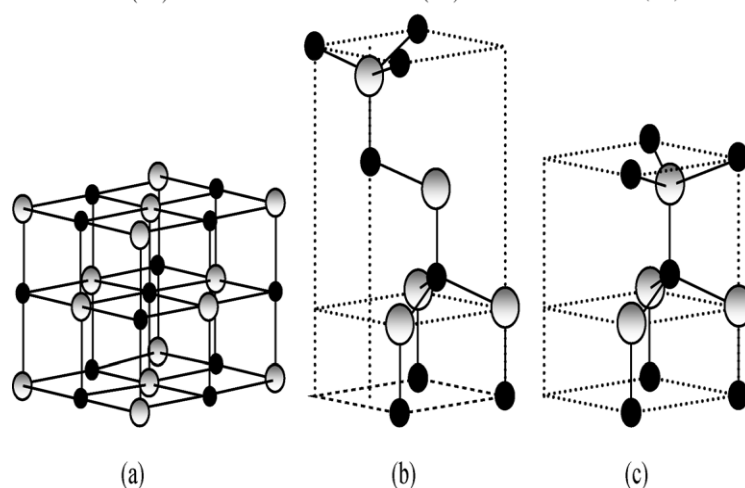


Figure 1.3. Schematically representation crystal structures of ZnO: (a) Rochelle salt or cubic rocksalt, (b) cubic zinc blende, (c) hexagonal wurtzite, gray spheres denote Zn atoms, and black spheres denote O atoms

This tetrahedral coordination is typical of  $sp^3$  covalent bonding nature, where four cations are surrounded each anion at the corners of a tetrahedron, and vice versa. as represented in Figure 1.3, that gray spheres denote Zn atoms, and black spheres denote O atoms, but these materials also highly great ionic properties that tends to increase the band energy gap beyond the one expected from the covalent bonding.

Copper has two stable oxides, cuprous oxide ( $Cu_2O$ ) and cupric oxide ( $CuO$ ). Both of them have major important, wide range of application and specific properties. The first oxide of copper is cuprous oxide ( $Cu_2O$ ) which is an important p-type semiconductor material, it has the major applications of  $CuO$  are use as transparent active p-type layers performance in conversion light to electrical energy in solar cells, field effect touch screens, transistors, and gas sensors. In addition, other applications in photo catalysis, photo electrochemical water splitting, solar energy conversion, biosensors, and coherent propagation of excitons. Especially, the resulting of high electro catalytic activity from multi electron oxidation mediated in enzyme-free glucose sensors by surface metal oxide layers. and they play an important role in the selective surface modification for example

passivation, hardening, coloration in the form of coatings of various substrates. Although, studied numerous nanostructure of  $\text{Cu}_2\text{O}$  materials with difference morphologies, such as nanowires, nanoparticles, nanocubes, nanosheets, hollow nanostructures and nanospheres, moreover, the high crystalline  $\text{CuO}$  nanofilms have been prepared by spin coating and annealing combined with a simple chemical method (Feng et al. 2014).

The second oxide of copper is cupric oxide ( $\text{CuO}$ ) it has p-type direct bandgap (1.4 eV) semiconductor due to copper vacancies in the structure. With unique characterization, useful photocatalytic properties and photovoltaic properties, particularly, and special properties include low production cost, non-toxic, electrochemical activity, abundance constituents in nature and chemical stability, in addition, possess significant role in the studies of metal semiconductor (MS), metal interlayer semiconductor (MIS), in the last decades Schottky diodes. Thus, by inserting an interlayer between the semiconductor and metal, the interfacial layer can be modified electrical parameters of metal semiconductor structures (Erdoğan et al. 2010). Moreover, large various applications such as gas sensors, catalysis, bio sensing, high temperature superconductors, magnetic storage media, solar cells, batteries, electronics, electrode materials, field of emissions and lithium-ion electrode materials numerous development technique and methods have been used to synthesis  $\text{CuO}$  nanoparticles including catalysis electrodeposition, spin-coating, sol-gel, gas sensors, solvothermal, hydrothermal and thermal oxidation, heat transfer fluids, and surface enhanced Raman spectroscopy. Although reported countable publications on the photocatalytic and as an antimicrobial activity of  $\text{CuO}$  nanostructures (Sathyamoorthy and Mageshwari 2013).

Cuprous oxide ( $\text{Cu}_2\text{O}$ ) is one of the well-known p-type narrow direct band gap 2.1 eV semiconductors. It has many advantages of non-toxicity, low cost and abundance of its starting material. It has large application include of solar cells, photo catalysis, and photo electrochemical water splitting, due to its favorable absorption in the visible range. The two materials have a special relative position of the energy band, which is the conduction band minimum (CBM) of  $\text{Cu}_2\text{O}$  is a little higher than the conduction band minimum (CBM) of  $\text{ZnO}$ , and the valance band maximum (VBM) of  $\text{Cu}_2\text{O}$  is lower than the valance band maximum (VBM) of  $\text{ZnO}$ , therefore, These properties allowed that the p-n heterojunction of  $\text{Cu}_2\text{O}/\text{ZnO}$  has significant applications in optoelectronics, electrics, and



fields of nanotechnology. The heterojunction of Cu<sub>2</sub>O/ZnO was successfully prepared by ease steps of electrodeposition, the electrodeposition presents many advantages, it requires a simple, low cost apparatus, and the deposition is realized at low temperature and at atmospheric pressure, and also, the film thickness can be controlled by the charge consumed during the deposition process. Thus, the produced Cu<sub>2</sub>O/ZnO heterojunction by electrodeposition is favorable to construct a facile and robust photo electrochemical sensor. Moreover, Cu<sub>2</sub>O/ZnO heterojunctions can absorb high visible light and have greater photo electrochemical performances in electron transitions and carrier effective separations than that of single zinc oxide (Li et al. 2014).

Semiconductor of cuprous oxide (Cu<sub>2</sub>O), with special magnetic and optical properties, has attracted increasing attention in different application include potential photovoltaic material, photocatalysis reactions, solar energy conversion, photocurrent generation, a stable catalyst for photo activated splitting of water or other liquids under visible light irradiation. Finally, both CuO and Cu<sub>2</sub>O nanospheres can be used for gas sensing. Cu<sub>2</sub>O nanostructures, nanocrystals or cuprous oxide film with different structures, size and surface morphologies such as nano rods, nano cubes, nano octahedron, and nano spheres, have been synthesized by various methods such as vacuum evaporation, wet chemical, thermal relaxation, electrodeposition, solvothermal method, complex precursor surfactant assisted route, and their surface-dependent catalytic, electrical and other properties have been studied (Kandjani et al. 2015).

Cu<sub>2</sub>O can be prepared by non-vacuum techniques, such as thermal oxidation of Cu sheets and electrochemical deposition (ECD). It is a native p-type semiconductor, due to a high concentration of negatively-charged copper vacancies; this is combined with a high absorption coefficient for energies. High majority carrier mobility (in the range of 100 cm<sup>2</sup>/Vs), and also large minority carrier diffusion length up to several micrometers (Malerba et al. 2011). Several techniques and methods have been used for synthesizing cuprous oxide (Cu<sub>2</sub>O) films with both high and low temperature contain thermal oxidation, hydrothermal, reactive magnetron sputtering, and electrodeposition (Abdellah et al. 2016).

P-type conduction property of  $\text{Cu}_2\text{O}$  is due to the formation of Cu vacancies and delocalized holes after the removal of copper atoms from the lattice through oxidation reaction as shown these two reactions: (Nolan et al. 2006).



It is clearly seen that reaction (1.2) depends on the  $\text{OH}^-$  concentration (i.e. pH) of the bath. At low pH values presence of excess  $\text{Cu}^+$  ions may favor the formation of Cu rich or O deficient (i.e. having O vacancies)  $\text{Cu}_2\text{O}$  films. Thus high density of donors can be expected and therefore the film may become n-type (Siripala 2008). When the pH of the electrolyte is higher and lower concentrations of Cu ions, there will be a tendency to produce  $\text{Cu}_2\text{O}$  films with Cu vacancies. In other words, acceptor density will become significant and then the films become p-type. It is clear that the  $\text{OH}^-$  concentration value (pH) does not independently determine the conduction type but according to equation (1.2) it should depend on the concentration of the ( $\text{Cu}^+$ ). On the other hand, it is important if there is a possibility of controlling the defect concentration of the  $\text{Cu}_2\text{O}$  film by the pH of the depositing bath and the ( $\text{Cu}^+$ ), concentration, This is important because  $\text{Cu}^+$  vacancies produce p-type conductivity while oxygen vacancies could produce n-type conductivity in  $\text{Cu}_2\text{O}$  films (Jayathileke et al. 2008).

Co-doping is an effective method for synthesis p-type conductivity in zinc oxide and also to decrease the band gap of its. In this process the layer of ZnO could be doped for rising and improving semiconducting properties. The term of co-doping means that along with the acceptors that are incorporated to produce holes, donors are also incorporated during the growth (Janotti et al. 2009). In addition, depositing a moderate bandgap semiconductor on zinc oxide increases the absorption of visible light. Such semiconductor is cuprous oxide  $\text{Cu}_2\text{O}$ , an abundant, non-toxic and medium direct bandgap of energy, copper acts as a good acceptor for zinc oxide. It can be used to reduce the carrier concentration in n-type ZnO by acting as a compensating center.  $\text{Cu}_2\text{O}$  has a direct band gap of 2.1 eV, high room-temperature mobility, poor cell performance is

found in  $\text{Cu}_2\text{O}$  heterojunctions, and a reasonable minority carrier diffusion length as single crystal for performance of solar cell (Dimitriadis. et al. 1983).

Furthermore, copper oxide is one of the significant candidates to form coupled semiconductors by using its narrow band gap that achieve larger photocatalytic activities in sunlight. The size of particle, crystal faces and crystallinity of  $\text{Cu}_2\text{O}$  are significant factors for determination of the p-n junction interface, therefore, it has an effect for synthesis to the heterojunction solar cell. The energy level distribution and density of interface states at the p-n junction can be affected by that difference and, therefore, also the unwanted recombination losses at the interface. In addition, various methods have been used to fabricate of p- $\text{Cu}_2\text{O}$ /n-ZnO heterojunction solar cells, such as sputtering aluminum doped ZnO film on to electrodeposited  $\text{Cu}_2\text{O}$  thin films (Noda et al. 2013), and depositing ZnO thin films on high-quality thermally oxidized copper sheets, electrodeposition could provide high quality films with some advantages including material stability because of low temperature deposition conditions, better crystallinity, and also higher conductivity. Among nanoparticles metals copper and copper oxide nanoparticles promising best candidate in modern technologies and is readily available applications (Chen et al. 2011).

In this thesis study, ZnO films decorated with  $\text{Cu}_2\text{O}$  nanocubes were prepared by practical electrochemical method, based on the underpotential deposition (UPD). A detailed characterization of ZnO films decorated with  $\text{Cu}_2\text{O}$  nanocubes was performed. It was reported that a systematic study of the influence of  $\text{Cu}_2\text{O}$  nanocubes doping on the structural, optical and photoelectrochemical characteristics of ZnO films.

## 2. LITERATURE SUMMARIES

Environmental contaminants in water have a serious threat to human health and safety of public. The scientist and researchers tried several efforts to solve this crisis by degrading environmental contaminants, they found photocatalysis, which is a development technology, various types of photocatalysts, particularly the semiconductor photocatalysts (e. g., ZnO and TiO<sub>2</sub>), are used in the treatment of environmental contaminants, with some advantages such as large-scaled easy synthesis and low-cost preparation (Ma et al 2016). Researcher's efforts in photocatalytic pollutant degradation and water splitting by using visible light that is abundant in the solar spectrum were to decrease environmental problems and produce sustainable energy sources. They used oxide of metals such as BiVO<sub>4</sub>, Bi<sub>2</sub>O<sub>3</sub>, WO<sub>3</sub>, Fe<sub>2</sub>O<sub>3</sub>, and Cu<sub>2</sub>O as photocatalysts with visible-light activities. Semiconductors photocatalysis techniques have been used for water splitting and pollutant degradation, because of its great capability of converting light energy into chemical energy. Photocatalysis has attracting special important economically and environmentally safe option for solving pollution problems and energy. Since the discovery of photocatalytic splitting of water on a TiO<sub>2</sub> electrode in 1972, various semiconductor photocatalysts have been shown to carry out chemical reactions under light illumination, among various semiconductors showing photocatalytic activity, wide band gap semiconductors such as ZnO, TiO<sub>2</sub>, etc. a big hope in helping ease the energy and environment crisis through effective utilization of solar energy based on photovoltaic and water-splitting devices (Zhang et al. 2014).

Photocatalysis is a well-known technique for the degradation of inorganic and organic pollutants in air and water, various photocatalysis have been studied such as CdS, TiO<sub>2</sub>, and ZnO, Fe<sub>2</sub>O<sub>3</sub>. Among them zinc oxide (ZnO) is a well-known n-type semiconductors in II–VI group, with a hexagonal wurtzite crystal structure, its excellent photocatalytic efficiency and good stability due to its wide direct band energy gap of 3.37 eV at 300 K and a higher exciton binding energy of 60 meV at room temperature, on the other hand.

exhibits a unique physical and chemical properties, high specific surface area, high electrical conductivity, high isoelectric point (IEP) of about 9.5 (Mohd et al. 2014), high aspect ratio, low-dimensional volume, light-matter interaction, cost-effectiveness, lower cost material due to abundance in nature, therefore, it have high chemical and mechanical stability, non-toxicity, However, the photocatalytic activation of zinc oxide is used to eliminate and reduce nocuous species takes place only under UV illumination (Nawar et al. 2014).

Noble metal nanoparticles, such as Pd, Au, Pt and Ag, are large effective oxidation catalysts that make them of use as active materials to improve the reactions take part on surfaces of gas sensor. Thus, numerous techniques have been studied to introduce noble metal additives onto oxide semiconductors. Consist of impregnation, sol– gel, sputtering and thermal evaporation, after the functionalization, different gas sensors with improved behaviors were produced (Liu et al. 2012).

Furthermore, zinc oxide promise practical applications in the area of nanoscale laser diodes and ultraviolet (UV) sensors. Because of the radial quantum confinement effect of nanowires, zinc oxide nanowires possess high density of states at the band edge. It has been showed that UV lasing nano-devices working at room temperature with a low-lasing threshold depended on zinc oxide nanowires would be quite potentially feasible. Lyu et al. (2003) reported and demonstrated vertically well-aligned zinc oxide nanowires on sapphire substrates or zinc oxide nanoneedles on silicon substrates at low-temperatures ranging from 400 to 500 °C using metal-organic chemical vapor deposition.

Zinc oxide is possess an n-type transparent semiconducting material at room temperature (300K) for photovoltaic application, In addition, special nanostructures characterization include growth properties, optical properties, and electrical properties, thus, the potential for optoelectronic devices depend on it, On the other hand, zinc oxide has small transmittance at the wavelength of light reported for utilizing solar energy conversion, given that the solar spectrum is in the 250-2500 nm region and the in the infrared region light is 780-2500nm. Generally, zinc oxide is a high performance material when it comes to easy deposition to high qualities, low resistivity, high mobility and challenges regarding solar cell applications (Gao et al. 2011).

In the electrochemical deposition field zinc oxide thin films have been deposited with various methods and techniques. Some of them are pulsed laser deposition (PLD), chemical vapor deposition (CVD), spray pyrolysis, reactive magnetron sputtering, sol-gel method and molecular beam epitaxy. Therefore, zinc oxide materials have been successfully synthesized with different sizes and morphologies, including: nanowires, nanorods, nanotubes, nanofibers, nanobelts (Lin et al. 2015).

The optical properties of metal for example potassium (K) doped zinc oxide (ZnO) thin films deposited onto glass substrate by chemical bath deposition (CBD) technique is investigated. This technique has many advantages such as simplicity, low cost, large area films with good uniformity. The crystallinity, surface morphology and the element composition of the thin films were studied. The optical behavior of K-doped ZnO thin films were investigated by optical transmittance spectrum and photoluminescence (PL) studies. The synthesis of potassium doped zinc oxide nanofilms by sol-gel dip-coating method has been reported, and they had demonstrated the optical properties and the evolution behavior under different annealing temperatures. They focused to synthesize K-ZnO doped thin films by chemical bath deposition technique and effective of K-doping on the surface morphology and optical properties such as optical energy band gap, extinction coefficient, refractive index, dielectric constant, absorption coefficient and photoluminescence (PL) of ZnO thin films, thus, the energy band gap value determined from the optical transmittance spectrum decreases with the increase in the doping concentration (Krishnan and Ranganathan 2013).

Many types of 1D ZnO nanostructures have been prepared. Recently, 2D ZnO nanodiscs or nanosheets have also been synthesis by thermal oxidation of zinc/ZnS powders or by carbon-thermal oxidation and carbon-thermal reduction of zinc oxide powders. These two vapour phase methods are limited by their low yield of temperature because they need high temperature over than 1500 °C. Moreover, the weak or not observation of UV emission of ZnO nanosheets at room temperature is appeared (Cao et al. 2005). In contrast, soft environments on a large scale required carrying out the solution phase method, they used electrochemical deposition under specific conditions for preparation of 2D ZnO nanoplates in conjunction with nanorods. Over the past decades, one-dimensional (1D) ZnO nanostructures (nanowires, nanotubes, nanosheets and nanobelts)

have attracted a great deal of research interests, various physical and chemical methods have been developed for the synthesis of 1D nanostructured metal-oxides such as hydrothermal, ultrasonic irradiation, electrospinning, anodization, sol-gel, molten-salt and carbothermal reduction, etc. (Lin et al. 2015).

Electrodeposition is a process as a low cost, low temperature, and thin film synthesis method. Those compounds that related to the formation of photovoltaics (PV) have been successfully grown using electrodeposition since the 70's. Kroger et al. (1978) reported that co-electrodeposition as a classic methodology used for CdTe deposition in his work. The co-electrodeposition technique is simple, low-cost and given the right solution chemistry. This method has been formed many binary compounds at a controlled potential or current in a single solution containing precursors for both elements. The transition metal oxides such as (Fe, Co, Ni, and Cu) had been used, on the other hand, the innovation of thin film lithium batteries with high storage capacity and cost-effective anode materials, because these materials have the ability to reverse store high Li through a heterogeneous conversion reaction. The key challenge for CuO and Cu<sub>2</sub>O practical use in thin film lithium batteries is the improvement of their high rate capacity and cycling performances (Barreca et al. 2012).

Cu<sub>2</sub>O nanostructures, nanocrystals or cuprous oxide film with different structures, size and surface morphologies such as nanorods, nanocubes, nanooctahedron, and nanospheres, have been synthesized by various methods such as vacuum evaporation, wet chemical, thermal relaxation, electrodeposition, solvothermal method, complex precursor surfactant assisted route, and their surface-dependent catalytic, electrical and other properties have been studied (Kandjani et al. 2015). Copper oxide (CuO) films of p-type band gap, possess an important role in the transparent conducting oxides (TCO) due to their great applications in optoelectronic devices, a basic prerequisite for a TCO is that it meets two important characteristics of optical transparency and electrical conductivity. Since NiO was found as the first p-type transparent conducting oxide, many efforts done to produce new p-type oxides, thus many p-type oxides of semiconductors have been studied. For example, CuAlO<sub>2</sub> as another p-type transparent conducting with considerable improvement over NiO, and also SrCu<sub>2</sub>O<sub>2</sub> was reported to have optoelectronic properties superior to those of CuAlO<sub>2</sub>. Moreover, in last decade studied CuO films use yet another

P-type TCO with some advantages such as nontoxicity, narrow direct bandgap, good transparency, and possibility of deposition at low temperature. In addition, the major applications of cupric oxide (CuO), are used as transparent active p-type layers in solar cells, field effect touch screens, transistors, and gas sensors. The surface morphology and structure of the films was found that playing significant role in the optical performance. Thus, the fabrication of CuO films on different substrates has been extensively studied recently. For example, the seed layer assisted chemical bath deposition of CuO films on ITO-coated glass substrates with notable morphology and crystallinity. And also, the CuO films coating on n-Si substrate by photo electrochemical properties. On the other hand, the structural, optical and electrical properties of CuO films on microscope glass slides chemically deposited, according to these reports clarify that the copper oxide films deposited on different substrate and various performances also be a suitable for deposition on glass substrates (Khan et al. 2016).

Cuprous oxide (Cu<sub>2</sub>O) has broad applications in photo catalysis, solar energy conversion, biosensors, photo electrochemical (PEC) water splitting, photocatalysis, photovoltaic (PV) cell, and PEC CO<sub>2</sub> capture and coherent propagation of excitons due to a direct band gap of approximate 2 eV. Cu<sub>2</sub>O generally exhibits as a p-type semiconductor (Yang et al. 2014). Researchers have been used developed various technique and method for obtaining the conductivity of Cu<sub>2</sub>O, Wijesundera et al. (2007) found that the Cu<sub>2</sub>O films have both n-type and p-type semiconductor, based on temperature, they explained that the cuprous oxide films behaved as p-type semiconductor when the annealing temperature is more than 300 °C, and behaved as n-type semiconductor when the annealing temperature is lower than 250 °C, on the other hand, the conductivity of cuprous oxide (Cu<sub>2</sub>O), also can be overcome by controlling the power of hydrogen value (pH) of plating solutions during electrodeposition process. A widely used approach to produce Cu<sub>2</sub>O film is electrodeposition, in which some strategies such as utilizing amphiphilic, ligating agents and tuning power of hydrogen (pH) value have been employ for controlling the orientation and surface morphology. On the other hand, polyol method is also used to synthesis oriented Cu<sub>2</sub>O films. Nevertheless, during this synthesis, surface capping agents, oxidants, reductants, and other additives required for controlling the growth of crystals and the surface morphology of the films. A development hydrothermal technique



used by Jayewardena et al. (1998) to prepare  $\text{Cu}_2\text{O}$  film with tunable morphologies and vacancy of Cu concentrations rely on situ redox reaction between Cu plate and  $\text{Cu}^{2+}$  ions.

Cu foil in HCl or  $\text{CuSO}_4$  solution at 40 °C treated by Fernando et al. (2000) and produced  $\text{Cu}_2\text{O}$  film by oxidation/reduction reaction between Cu and  $\text{Cu}^{2+}$  ions, this is an important idea because not require complex agents. With this consideration, modify the oxidation/reduction reaction by adopting hydrothermal treatment, facile development and template free synthesis of  $\text{Cu}_2\text{O}$  film. In addition, the effect of different anionic groups ( $\text{Cl}^-$ ,  $\text{NO}_3^-$ , and  $\text{SO}_4^{2-}$ ) on the shape transformation of  $\text{Cu}_2\text{O}$  has been reported (Pan et al. 2013).

McShane and Choi (2009) deposited n-type  $\text{Cu}_2\text{O}$  film in a cupric acetate solution at pH 5 by electrodeposition method and explained the effect of dendritic branching growth of cuprous oxide ( $\text{Cu}_2\text{O}$ ) crystals on the photocurrent of films. Tsui and Zangari(2013) studied the electrodeposition of n-type cuprous oxide  $\text{Cu}_2\text{O}$  film on  $\text{TiO}_2$  nanotubes in a cupric acetate solution at pH 5 for fabrication of photo electrochemical solar cells. Zhao et al. (2011) electrodeposited  $\text{Cu}_2\text{O}$  film in a cupric acetate solution, thus, they demonstrated the effects of reaction time, deposition potential, and solution temperature on the morphologies of n-type  $\text{Cu}_2\text{O}$  films. On the other hand, Golden et al. (1996) studied electrodeposition of p-type  $\text{Cu}_2\text{O}$  films in a cupric sulfate solution on stainless steel at pH 9. And also Jongh et al. (1999) at pH 9 they studied electrodeposition of p-type  $\text{Cu}_2\text{O}$  films in a cupric sulfate solution on fluorine doped tin oxide (FTO) glass. In another researcher efforts p-type  $\text{Cu}_2\text{O}$  film in a cupric sulfate solution at pH 7–9 were deposited by electrodeposition method and studied the effect of pH value on the carrier concentration of p-type  $\text{Cu}_2\text{O}$  bulk by Jiang et al. (2013). However, in current methods, the p-type  $\text{Cu}_2\text{O}$  films can only be fabricated in basic solutions and the n-type  $\text{Cu}_2\text{O}$  films can only be fabricated in acid plating solutions. It is not easy and hinders the synthesis of  $\text{Cu}_2\text{O}$  films with p-n homo junctions, due to requirement of two steps process in two solutions types (Yang et al. 2014). Furthermore, Scanlon and Watson (2011) have been showed the various interstitial sites of H residence in cuprite and they found that strong bound complex between hydrogen forms with copper vacancy. Moreover, the hydrogen is found to prefer not to occupy the center of the vacancy, but to move away from the center closer to one of the two oxygen anions.

There are two main factors limiting the use of  $\text{Cu}_2\text{O}$  materials in photocatalysis, the first of the limiting factors is poor stability in aqueous solution, this problem solved by using of some methods, such as locating protective layers of  $\text{CuO}$  or  $\text{Cu}$ , or even locating multi-protective layers of  $\text{ZnO}/\text{Al}_2\text{O}_3/\text{TiO}_2$  to enhance the stability of  $\text{Cu}_2\text{O}$  photocatalysts (Ma et al 2016). And the other limiting factor for  $\text{Cu}_2\text{O}$  photocatalysts is that  $\text{Cu}_2\text{O}$  exhibits poor photocatalytic performance because of its short electron diffusion length and low hole-mobility. Therefore, various approaches have been proposed to improve its photocatalytic activity, including control of morphologies and defects of  $\text{Cu}_2\text{O}$ , load of noble metals, combination with other semiconductors and carbon materials.

As a new anode material for lithium ion batteries,  $\text{Cu}_2\text{O}$  thin films were prepared by electrodeposition technique (Fung et al. 2004). Copper oxide was successfully electrochemically deposited with the pure cubic phase. The results of the combined electrochemical cell tests indicated that the electrodeposited copper oxide film had high electrochemical capacity and allowed excellent cycle retention. After 50 cycles, it was observed that the capacities were still sustainable at about 220 mAh/g and that the decay was not significant except for the first cycle. The  $\text{Cu}_2\text{O}$  film, dense and homogeneous by the electrochemical deposition, was successfully deposited on the  $\text{Pt}/\text{Ti}/\text{SiO}_2/\text{Si}$  layer without any subsequent heat treatment. SEM and TEM observation showed good adhesion properties between the film and substrate.

The transparent p-type  $\text{Cu}_2\text{O}$  thin film was produced by a process comprising a thermal reaction, deposited on a glass substrate, with a thickness of 50 nm, successfully (Sato et al. 2012). When the  $\text{Cu}_2\text{O}$  transparent thin film absorption spectrum was evaluated, it was 2.3 eV.  $\text{Cu}_2\text{O}$  films were prepared on flexible copper and Mo substrates in a basic environment by electrochemical deposition (Mathew et al. 2011). Such deposited films showed that the films contained only  $\text{Cu}_2\text{O}$  phase by p-type and XRD analysis. The thicknesses of the films are calculated from the interference fringes of the reflection spectra.  $\text{Au}/\text{Cu}_2\text{O}$  Schottky diodes were prepared by spraying  $\text{Cu}_2\text{O}$  films on Mo substrate as a layer of very pure gold with a thickness of 15 nm. Possible optical transitions near the tape edge were calculated from the spectral response of the device. It showed that there is a linear dependence of temperature on the calculated tape gap at different temperatures. The direct transition temperature dependence of 2.493 eV

observed at room temperature is shown. Electrodeposition is a suitable method for preparing Cu<sub>2</sub>O films on wide area substrates.

Growth of Cu<sub>2</sub>O thin films was investigated on the FTO surface by electrochemical deposition (Ryu et al. 2014). The effect of annealing temperatures and annealing times on the morphological, structural, photo electrochemical and optical properties of Cu<sub>2</sub>O thin films formed with pH value 11 was investigated. Cu<sub>2</sub>O thin films at pH 11 show higher photoconductivity. It has been found that the properties of these Cu<sub>2</sub>O thin films depend on the degree of crystallization and morphology. Cu<sub>2</sub>O thin film with the best structural and photoelectrochemical properties was obtained at 200°C annealing time in vacuum for 30 minutes. In this case, the highest (111)/(200) XRD peak intensity ratio of annealed Cu<sub>2</sub>O thin films is 52.5 and the highest photo acid density is 2.90mA/cm<sup>2</sup>. Cu<sub>2</sub>O thin films with adjustable growth orientations on glass and silicon surfaces were prepared using reactive sputtering and crystal growth investigated (Pierson et al. 2014). The effect of certain orientations on subsequent crystal growth during the growth phase of crystal growth, which was initially observed, has been studied in detail. Among various coating conditions, it has been found that the total pressure has a strong influence on the preferential orientation of Cu<sub>2</sub>O films. Cu<sub>2</sub>O thin film can be formed independently of deposition conditions. Provided that it has a sufficient thickness, this layer may be applied after exposure to air which acts as a core layer that determines the crystal orientation of a second layer that accumulates without a specific cleaning on its surface prior to application. High-resolution transmission electron microscopy analyzes demonstrate that a homo epitaxial growth occurs with the core layer, which has a microstructure consisting of single crystal groups.

In studying the preparation and application of CuO nanowires (NWs), the mean length of CuO NWs was found to increase from 0.4 μm to 2.8 μm and 6 μm, respectively (Chang et al. 2011). After oxidation, the initial copper film thickness increased from 0.5 μm to 1 and 2 μm. At the same time, CuO is p-type, so CuO NWs resistance is increased with increasing relative humidity. Furthermore, it can be seen that with a larger copper film thickness at the beginning and thus an average longer CuO NW length, the samples could provide a larger sensor response. CuO nanoparticles were prepared by thermal decomposition and characterized by XRD, TEM and UV-Vis spectroscopy (Dolui et

al.2013). And also nanoparticles are promising antioxidants in polymer processing and non-biological systems. The antibacterial activity of CuO nanoparticles has been tested against several bacterial groups with genetic differences. With increasing concentration of CuO nanoparticles, there is a significant reduction in bacterial growth. CuO nanoparticles exhibited bactericidal activity against *Escherichia coli* (bacterial infection in large intestine) and *Pseudomonas aeruginosa* with effective antioxidant activity. A very high level of formaldehyde-sensitive gas sensors consisting of CuO nanocouples were produced and characterized using various methods (Lee et al. 2014).

CuO nanocrystals were prepared by sequential ionic layer adsorption and reaction method which is a simple and low cost technique and the effect of deposition cycles on the physical properties of materials was investigated (Sathyamoorthy and Mageshwari 2013). Preparation conditions such as concentration, pH, adsorption, reaction and rinse duration are optimized to obtain homogeneous and high quality CuO thin films on glass surfaces. XRD studies have shown that all films exhibit multicrystalline properties with a monoclinic crystal structure. Here the characteristic vibrational mode of Cu-O is defined. Scanning electron microscopy (SEM) studies have shown that elongated particles of bar-shaped particles are formed by scattered growth. XRD, FTIR and Raman studies confirm the monocrystalline and single phase formation of CuO thin films. CuO nanocrystals with photocatalytic properties were prepared using an electrochemical method (Mukherjee et al. 2011).

Cu<sub>2</sub>O/CuO nanostructures were prepared by direct crystallization in the presence of sodium borohydride without using any oxidant or surfactant (Li and Fan 2011). A study was conducted to quantitatively evaluate the effect of the electrode temperature on the optical and photoelectrochemical properties of Cu<sub>2</sub>O film (Lin et al. 2014). Three different temperatures (35, 50 and 65 °C) were taken into account. At temperatures ranging from 35 to 65 °C, in an alkali bath containing copper sulfate and lactic acid at -0,30 V. P-type Cu<sub>2</sub>O thin films were successfully prepared on copper foil substrates by electrochemical deposition. These films have distinct morphology and crystal structure. They exhibit different optical and electrical properties. The film deposited at 50 °C and at 65 °C, Cu<sub>2</sub>O film deposited at 35 nanoparticles have come to fruition. The energy level diagrams of the films have been examined. The film at 35 °C gave a much denser PL

signal than the films prepared at 50 and 65 °C. In addition, Raman spectroscopy was used to confirm Cu<sub>2</sub>O film compositions. The properties of the films are closely related to the composition of the film. And Cu<sub>2</sub>O thin films were prepared by precipitating a copper target on a quartz substrate in a mixture of oxygen and argon gas (Zhang et al., 2009). The effects of partial pressure of oxygen and gas flow rate on the properties of the films are investigated. The changing oxygen partial pressure leads to the synthesis of copper oxides Cu<sub>2</sub>O, Cu<sub>4</sub>O<sub>3</sub> and CuO with different microstructures. The gas flow rate was 80 sccm, and with constant oxygen partial pressure of  $6.6 \times 10^{-2}$  Pa, single phase Cu<sub>2</sub>O films can be obtained. The deposited Cu<sub>2</sub>O films were found to have a very high optical absorption in the visible spectrum below 600 nm and exhibited photocatalytic reactivity under visible light.

Copper and copper oxide thin films were prepared using an electrodeposition method in an acetate bath (Wijesundera et al. 2006). Voltammetric curves were used to investigate growth parameters such as potential for deposition, pH and temperature. Structural, morphological, optical and electronic properties of potentially dependent films were investigated by XRD measurements, scanning electron micrographs, absorption measurements. This study suggests that a single deposition chamber can be used to control both the Cu and Cu<sub>2</sub>O and Cu-Cu<sub>2</sub>O mixtures by controlling the deposition parameters. Studies show that single-phase Cu<sub>2</sub>O and Cu thin films can potentiometrically electroplate in the range of 0 to 300 mV Vs SCE and -700 to -900 mV Vs SCE potentials, respectively, an aqueous solution containing sodium acetate and copper acetate. It is possible to electro coat Cu and Cu<sub>2</sub>O at the same potential in the range of 400 to -600 mV Vs SCE.

Cu<sub>2</sub>O thin films were prepared using a reactive magnetron sputtering system (Zhang et al., 2013). Band spacing, refractive index, mobility, hole density and electrical conductivity in films are also investigated. Cu<sub>2</sub>O thin films are manufactured in rich N and rich O conditions. Films deposited under oxygen-rich conditions have narrow bandwidth and high electrical conductivity, while films produced under nitrogen-rich conditions exhibit broadband spacing and low electrical conductivity. The results of the density functional theory are presented to explain the gas dependence of the band gap. A theoretical model based on Fermi-Dirac statistics, High electrical conductivities are due

to the receiver levels below the Fermi level. Thin films were produced under rich N and O conditions. The optical and electrical properties of these films have been investigated with permeability measurements, band-interval simulations and refractive index calculations.

The production of copper and zinc nanocomposite with controllable sizes, shapes and surface properties is vital for exploring copper-zinc-based nano-oxides for different applications. The nanocomposite will be used as a potential transducer for various applications, i.e., energy storage devices and catalysis. There are numerous reports on chemically and physically prepared nanocrystalline copper-zinc based oxides. Furthermore,  $\text{Cu}_2\text{O}$  combined with some metal oxides could effectively overcome combination of photo generated electron and holes which severely affects the photocatalytic activity. Additionally, coupling ZnO with  $\text{Cu}_2\text{O}$  can form p-n heterojunction which can get the utmost out of sunlight and improve the efficiency of electron-hole separation and photocatalytic activities (He et al. 2016).

The  $\text{Cu}_2\text{O}/\text{ZnO}$  heterojunction has been produced by several techniques and methods, such as thermal oxidation, sputtering, pulsed laser deposition, chemical vapor deposition, and electrodeposition (Jeong et al. 2011). Photochemical deposition of CuO onto hydrothermally grown ZnO nanorods were used to synthesized The  $\text{CuO}/\text{ZnO}$  heterostructured nanorods. The morphology of  $\text{CuO}/\text{ZnO}$  heterostructured nanorods was controlled by modulation of various growth conditions and evaluated by XRD, SEM, XPS, EELS (electron energy loss spectroscopy), and TEM (Kim et al. 2012).

$\text{Cu}_2\text{O}$ -modified ZnO nanorods prepare by electrodeposition method. The time of deposition is controlled amount of  $\text{Cu}_2\text{O}$ . The effects of the deposition time on the morphological, microstructural, optical properties, and catalytic performance of the  $\text{Cu}_2\text{O}$ -modified ZnO nanorods have been demonstrated. It can be found that as the  $\text{Cu}_2\text{O}$  deposition time increases, the diameter and length of the nanorods decreased, which can be affected by electrolyte corrosion during the  $\text{Cu}_2\text{O}$  deposition process. Unfortunately, the ZnO absorption in the region of visible-light is very low due to its wide bandgap, to provide the absorption of zinc oxide into the visible region, narrow bandgap semiconductors, such as CdS, CdSe, and  $\text{Cu}_2\text{O}$ , have been used to construct

heterostructures with 1D ZnO. Cu<sub>2</sub>O is significant semiconductor with ZnO for p-n heterojunction due to its narrow energy band (Lee et al. 2014).

## **3.MATERIAL AND METHOD**

### **3.1. Materials Used in Laboratory Studies**

#### **3.1.1. Used Chemicals**

Zinc nitrate hexahydrate [ $\text{Zn}(\text{NO}_3)_2 \cdot 6\text{H}_2\text{O}$ ], potassium nitrate ( $\text{KNO}_3$ ), copper sulphate pentahydrate ( $\text{CuSO}_4 \cdot 5\text{H}_2\text{O}$ ), sodium sulphate ( $\text{Na}_2\text{SO}_4$ ), lactic acid ( $\text{C}_3\text{H}_6\text{O}_3$ ), sodium hydroxide ( $\text{NaOH}$ ), sulfuric Acid ( $\text{H}_2\text{SO}_4$ ), ethanol ( $\text{C}_2\text{H}_6\text{O}$ ), acetone ( $\text{C}_3\text{H}_6\text{O}$ ).

#### **3.1.2. Instruments and Devices Used in Work**

Precision balance: Denver Instrument SI-234

PH meter: Orian 3 Star

Ultrasonic mixer: Apple S 60 H

Deionized water device: Human Power 1

Electrochemical analyzer: CHI 6096 E

X-ray diffractometer (XRD): Rigaku Ultima IV

Scanning electron microscope (SEM): JEOL JSM-6510

Energy dispersive spectrometer (EDX): JEOL JSM-6510

UV-VIS-NIR spectrophotometer: Shimadzu UV-3600

Solar simulator: Solar Light 16S-002

#### **3.1.3. Materials Used in Electrochemical Studies**

Electrochemical processes that make up a significant part of the work; analyzed substance, solvent, electrolyte and an electrode from an electrochemical cell and an electrochemical device known as potentiostat/galvanostat. We need to pay attention to the selection of materials to be used for electrochemical studies. The particulars are mentioned below.



### 3.1.3.a. Properties and Specializing Solvent and Electrolyte

The potential of the solvent and electrolyte to be used in electrochemical operations. The solvent used is high electrical conductivity, very high purity, and a high degree of solubility. It should have dielectric constant, and should not enter into reaction. Thus, with starting electrochemical studies, it is first necessary to investigate the chemical and physical properties of the solvent in detail. In addition, if pure water is used as the solvent, must be distilled water or higher purity production ultrapure water systems use. Therefore, we used ultrapure water as solvent in our studies and this is GFL 2008 brand deionization system has been show in Figure 3.1.



Figure 3.1. The pure water system that use for ultra-pure water

### 3.1.3.b. The solutions

In our studies, we found that aqueous basic solutions containing 0.02 M  $\text{Zn}(\text{NO}_3)_2 \cdot 6\text{H}_2\text{O}$ , 0.2 M  $\text{KNO}_3$ , in the first step. And 0.02 M  $\text{CuSO}_4$ , 0.2 M  $\text{Na}_2\text{SO}_4$  and 0.3 M lactic acid solution, in the second step, such as an environment that prepared by semiconducting materials were used by electrochemical method. The pH of the solutions is 9 that prepared by adjusting with pH meter using  $\text{NaOH}$  and  $\text{H}_2\text{SO}_4$ .

### 3.1.3.c. Electrochemical Cell

Electrochemical reactions can be performed in cells with two or three electrodes. Both of the cathode electrodes and anode electrodes are immersed in an electrolyte solution. Thus, the oxidation/reduction (redox) reactions take place, it's clear that the reduction reactions take place in the cathode electrode, and also the oxidation reactions take place in the anode electrode. In addition, usually the electroactive in cells consisting of three electrodes dissolving the compound and the electrolyte dissolved in the solution, the counter and reference electrode (Goodridge and King 1974). Another important factor is the use of unfractionated cells where the three electrodes are placed in separate compartments in electrochemical processes and the opposite, the study, in which the reference electrode is placed in one compartment as shown in (Figure 3.2).

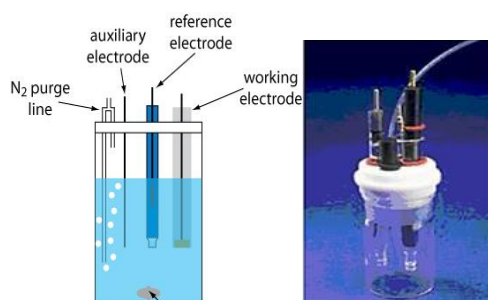


Figure 3.2. Electrochemical cell was used

### 3.1.3.d. Electrodes

Three types of electrodes are used: reference, counter and working electrode (Skoog et al. 1998). In electrochemical studies, one of the electrodes has a half-cell knowing and fixed potential, tis electrode having properties that it is independent of its composition of electrolyte desirable. It called reference electrode. These electrodes are used for potentially controlled electrolysis and voltammetry techniques; therefore, the reference electrode should be used in order to determine the potentials. And also the reference electrode must be stable, easily prepared, with a specified current range. It must behave reversely and should not change over time. Commonly reference electrodes are silver-silver chloride (Ag/AgCl) and saturated calomel reference electrode (SCE) used (Erdoğan 2009).

In our studies, SCE for the electrochemical preparation of copper oxide materials, Ag/AgCl reference electrode was used in photoelectrochemical studies. Calomel electrode is very easy to prepare because of the ease of preparation of analytical chemists an electrolyte mercury-mercury chloride reference electrode; mercury and calomel in ( $\text{Hg}_2\text{Cl}_2$ ), potassium chloride (KCl) solution formed into a platinum wire for external connection. A submerged half-cell is used as shown in (Figure 3.3). With this half-cell, temperature and potassium chloride depending on the concentration of the reference electrode.

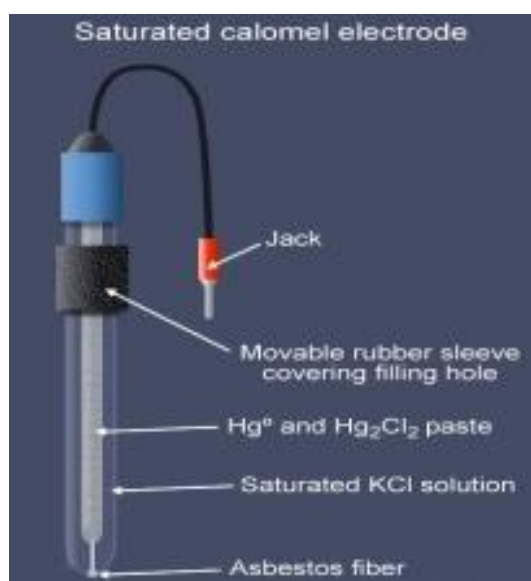


Figure 3.3. Saturated calomel electrode

The Saturated calomel electrode is 0.224 V due to faulty connection potential in case of potential connection to standard hydrogen electrode, liquid connection. However, when there is no fluid connection, this value is around 0.241 V (URL-1 2015). Figure 3.4 shows the potential change as a function of temperature. The potential values of the calomel electrode versus the standard hydrogen electrode (SHE) at 0-100 ° C,

$$E_T = 0,244 - 0.00072 (T - 25) \quad (3.1)$$

According this Equation (3.1) the potential change as a function of temperature as shown in Figure 3.4 at (12-50 K), on the other hand, the potential of the reference electrodes can change over the time, it should be preserved in a solutions.

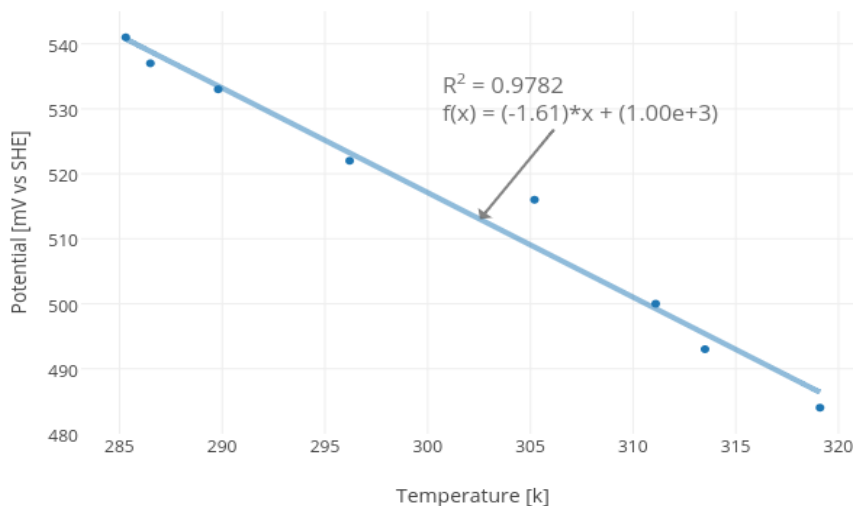


Figure 3.4. Change of electrode potential with temperature

The Ag/AgCl reference electrode was obtained by immersing Ag in an agitated solution after agglomeration with AgCl in the electrolytic solution (Figure 3.5)

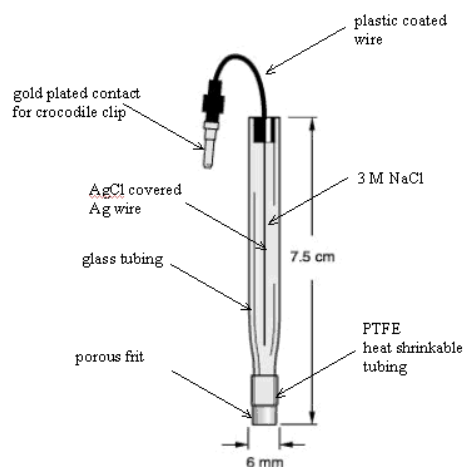


Figure 3.5. Ag/AgCl reference electrode

The potential of Ag/AgCl electrode is 0,222 V against standard electrode potential SHE. This value for SCE is 0.268 V. On the other hand, the concentration of KCl affects the electrode potential for both Ag/AgCl and SCE. For example, when the molar concentration of KCl for the calomel electrode is taken as 1.0 and 0.1 M, the voltages at 25 ° C are 0.282 and 0.334 V, respectively. Generally, Ag/AgCl electrodes can be used when working above 60 °C with calomel electrodes.

The working electrode is the most important part of the electrolysis system. On the other hand, the counter electrode has no effect on the reaction occurring in the working electrode. And also the counter electrode is used to complement the circuit and feeds the working electrode with electrons. In addition, a small current is observed in the counter electrode due to the non-process electrolyte types in the working electrode. Therefore, the counter electrode process is not interested. Many uses of platinum wire as counter electrode are due to its inert nature in electrochemical studies as shown in (Figure 3.6).



Figure 3.6. Platinum counter electrodes

The working electrode is the electrode at which the analyte is oxidized or reduced. The potential between the working electrode and the reference electrode is controlled. Electrolysis current passes between the working electrode and a counter electrode. The working electrode acts as an anode material in which an oxidation reaction takes place during oxidation in an electrochemical cell, and also cathode material during which the reduction reaction takes place during reduction. Moreover, the preference of the cathodic and anodic working electrode is important (Weinberg 1972). For this reason, surface morphology and activity must be taken into account in the preference of the electrode material. In our studies, ITO (indium tin oxide) coated glass was used as the working electrode, platinum wire was used as the counter electrode, and Ag/AgCl and SCE were used as the reference electrode.

### 3.1.3.e. Potentiostat

Potentiostat is an electronic device that adjusts the potential of the working electrode versus the reference electrode. This is used in potentially controlled electrolysis. The linearly scanned potential generator, similar to the integration circuits, is the signal source as shown in Figure 3.7.

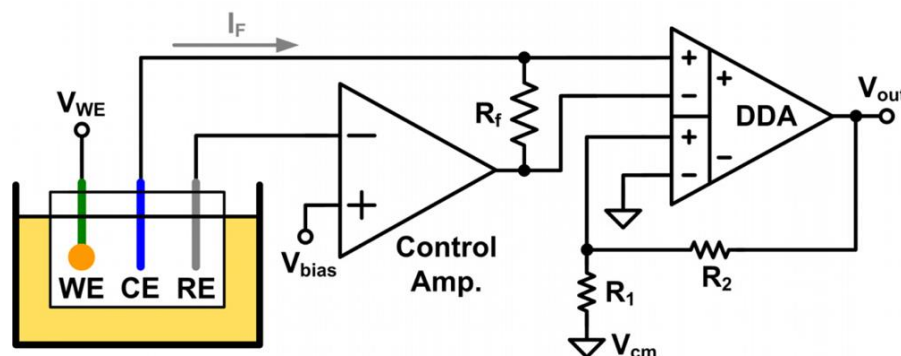


Figure 3.7. Schematic representation of potentiostatic components used in electrochemical studies

The output signal from the source first comes to the potential control circuit. And also the electrical resistance is very large ( $> 10^{11} \Omega$ ) for a small amount of current flow in the control circuit containing the reference electrode, this ensures that all of the current from the source is transferred from the opposing electrode to the working electrode. In addition, in the potentiostat process, the current measuring circuit is connected to the working electrode. Moreover, the potential tracer connected to the reference electrode constantly indicates the potential of the electrode which it is connected. Although, the control circuit adjusts this current to ensure that the potential between the reference electrode and the working electrode is equal to the output potential of the linear voltage generator, The measured potential is the potential between the work and the reference electrode. Finally, during the test run the working electrode is at the known true potential and this potential is recorded as a function of time (Erdoğan 2009).

Photoelectrochemical studies were carried out with a CHI electrochemical analyzer (CHI 6096 E Inc., USA) in a three-electrode configuration with , indium tin oxide (ITO) coated glass as working electrode, Platinum wire (Pt) as a counter electrode, Ag/AgCl and standard calomel electrode SCE as the reference electrode. In our studies we used (CHI

6096E USA) type operational potentiostat in our studies (Figure 3.8). It alternating voltammetry through potentiostat, potentially controlled electrolysis and amperimetric techniques were used for analysis.

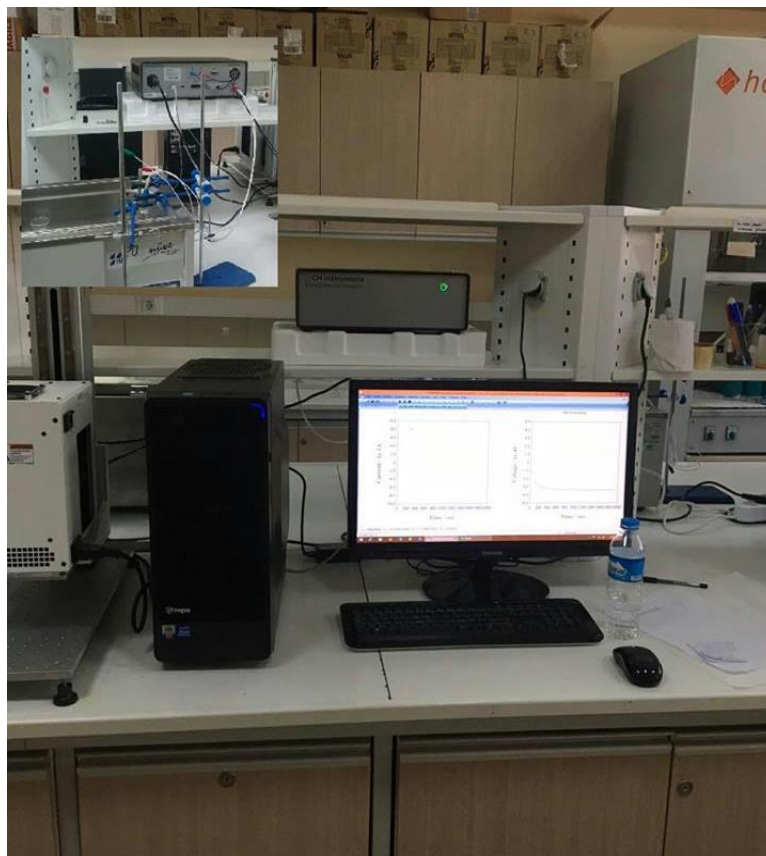


Figure 3.8. Schematic representation of the potentiostat system used in our studies

## 3.2. Methods Used

### 3.2.1. Electrochemical Methods

Voltammetry, an electroanalytical method used in electrochemistry, on the condition that a working electrode is polarized so that information about the analyte can be obtained, (Skoog et al., 1998), in which the flow is measured in the form of a potential function to be applied. To provide the voltammeter polarization, the surface area of the working electrodes is taken to be a few millimeters square, and a few micrometers square (Heyrovsky 1922). Using mercury electrode as a microelectrode is the most important difference that separates polarography, a special type of voltammetry, from other

voltammetric techniques. Voltammetry used for many analytical purposes, is widely used for non-analytical purposes. As an example, in the investigation of adsorption processes on the surface, examination of the oxidation / reduction processes occurring in various media, As elucidation of electron transfer mechanisms occurring on chemically modified electrode surfaces (Erdoğan 2009).

The cyclic voltammetry is increased in potential linearly as a function of time up to a certain potential value and returned to its starting potential again as shown in (Figure 3.9).

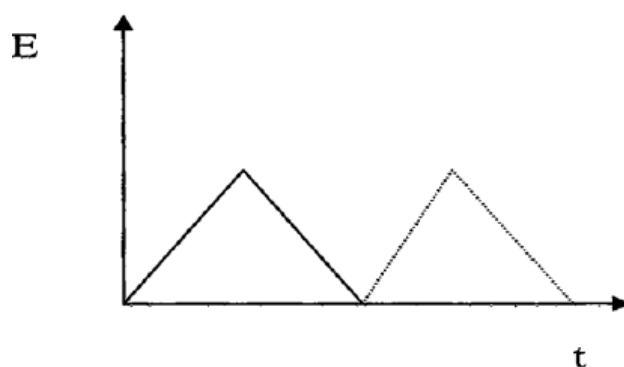


Figure 3.9. Cyclic voltammetric technique for conversion the potential vs time

The graphs of the potential versus current values obtained by using the alternating voltammetry technique are called voltamograms. Usually, electrochemical information is given in the form of these graphs (Malachuk 1969). Potential values and currents can be measured at the same time when the reaction occurs in an electrochemical cell. The potential of the working electrode is changed between the values determined in the negative and positive direction based on the potential of the reference electrode by means of a potentiostat. Electrode potential is scanned in the positive direction and a current is generated by the presence of molecules or ions in the environment reaching the oxidation potential. This flow is called the anodic current. If the electrode is to be scanned on a potentially negative side, a current will be generated due to the reduction of the electroactive substances when the ions or molecules in the environment reach the reduction potential, and the generated current is called the cathodic current (Skoog et al. 1998).



For a cyclic electrode response, there must be a voltage difference between the cathodic peak potential ( $E_{pc}$ ) and the anodic peak potential ( $E_{pa}$ )  $(0.059/n)$  V. The formal potential ( $E^\circ$ ) of the redox couple examined is equal to the midpoint of these two peak potentials. For an alternating voltamogram, the ratio of anodic peak current to cathodic peak current is approximately one ( $I_{pa} / I_{pc} \cong 1$ ).



For Equation 3.2, the amount of oxidant on the surface decreases with time, so the current will fall and the reaction will end. Thus, a selective reaction will be realized by adjusting potential. The reference electrode is used in addition to the working electrode and the counter electrode. According to the Nernst equation, as the concentrations of the electroactive substances change with time, the potential of the working electrode is always kept constant by using the potentiostat.

According to the Nernst equation (Equation 3.3) for Equation 3.2, the concentration of oxidant will decrease over time and will potentially change with time. The oxidant in the environment, it will remain at fixed value for the potential short-term with the exhaustion of the whole (Erdoğan 2009).

$$E = E^\circ - \frac{RT}{nF} \ln \frac{[\text{Red}]}{[\text{Ox}]} \quad (3.3)$$

$E_{\text{cell}}$  is the cell potential,

$E^\circ_{\text{cell}}$  is the standard cell potential,

R is the universal gas constant:  $R = 8.314472(15) \text{ J K}^{-1} \text{ mol}^{-1}$ ,

n is the number of moles of electrons transferred in the cell reaction or half-reaction,

F is Faraday constant, the number of coulombs per mole of electrons,

$F = 9.64853399(24) \times 10^4 \text{ C mol}^{-1}$ ,

T is the temperature in kelvins at room temperature (25 °C),

RT/F may be treated like a constant and replaced by 25.693 mV for cells.

### 3.2.2. UV-GB Spectroscopy

Molecular absorption spectroscopy is the method of measuring the absorbance ( $A$ ) or permeability ( $T$ ) of a solution in a cell by using the wavelengths. Absorption in the ultraviolet and visible region is mainly due to the stimulation of the bonding electrons in the molecules. As a result, the wave lengths of the absorption peaks with the types of bonds in the species studied and are thus used in the quantitative determination of functional groups in a molecule as well as of compounds carrying functional groups (URL-2 2015). The components of the double-light-path spectrometry are shown in Figure 3.10.

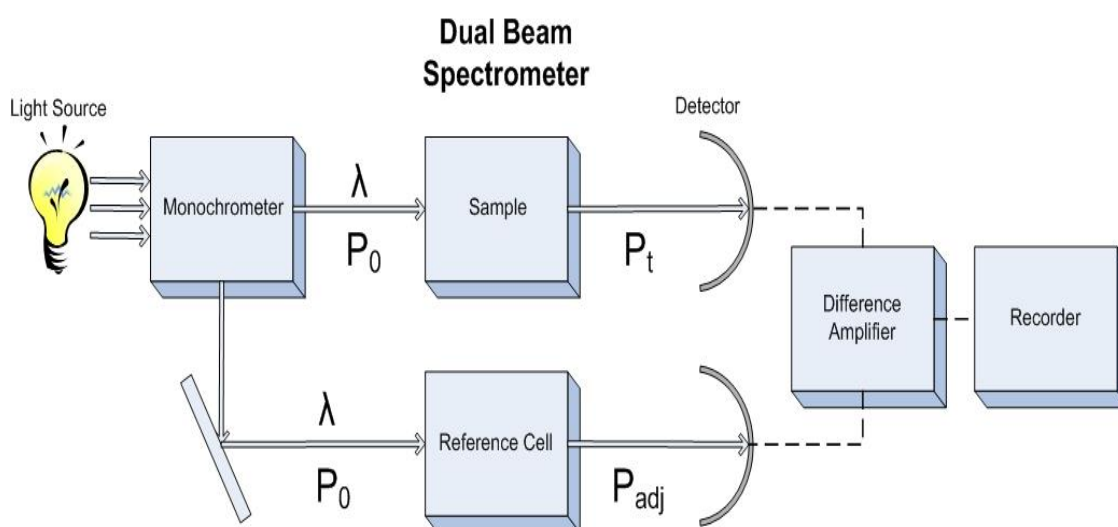


Figure 3.10. Schematically representation of double beam spectrometer

The components of the double-light-path spectrometry are shown in Figure 3.10. In the first the light comes from the light source to a monochromator. And then the light from the monochromator is sent to the reference and sample cells, separated by two equal wavelengths. These two light beams sent to the sample cell and reference cell are detected with two different detectors. Finally, the permeability value of the reference cell and the permeability value of the sample cell are continuously compared in the signal readout, and the ratio of the generated signals is read. The spectrophotometer used in our studies is shown in Figure 3.11.



Figure 3.11. Shimadzu UV-3600 UV-VIS-NIR spectrophotometer used in our studies

### 3.2.3. SEM

Scanning Electron Microscopy (SEM) is a powerful method for the investigation of surface structures of Molecules, This technique provides a large depth of field, which means, and the area of the sample that can be viewed in focus at the same time is actually quite large. SEM has also the advantage that the range of magnification is relatively wide allowing the investigator to easily focus in on an area of interest on a sample that was initially scanned at a lower magnification. Furthermore, the three-dimensional appearing images may be more appealing to the human eye than the two-dimensional images obtained with a transmission electron microscope. Therefore, an investigator may find it easier to interpret SEM images. Finally, the number of steps involved for preparing specimens for SEM investigation is lower and thus the entire process is less time consuming than the preparation of samples for investigation with a transmission electron microscope.

Essential components of all SEMs include electron column, scanning system, detector, display, vacuum system and electronics controls. Infrastructure requirements: power supply, vacuum system, cooling system beam condenser, vibration-free floor, room free of ambient magnetic and electric fields. SEMs always have at least one detector (usually a secondary electron detector), and also most have additional detectors as shown in

(Figure 3.12). The electron column of the SEM consists of an electron gun and two or more electromagnetic lenses operating in vacuum. The electron gun generates free electrons and accelerates these electrons to energies in the range 1-40 keV in the SEM. The purpose of the electron lenses is to create a small focused electron probe on the sample. Most SEMs can generate an electron beam at the specimen surface with spot size less than 10 nm in diameter while still carrying sufficient current to form acceptable image. Typically the electron beam is defined by probe diameter in the range of 1 nm to 1  $\mu\text{m}$ . In order to produce images the electron beam is focused into a fine probe, which is scanned across the surface of the sample with the help of scanning coils. Moreover, each point on the specimen that is struck by the accelerated electrons emits signal in the form of electromagnetic radiation. Selected portions of this radiation, usually secondary or backscattered electrons are collected by a detector and the resulting signal is amplified and displayed on a computer screen or computer monitor.

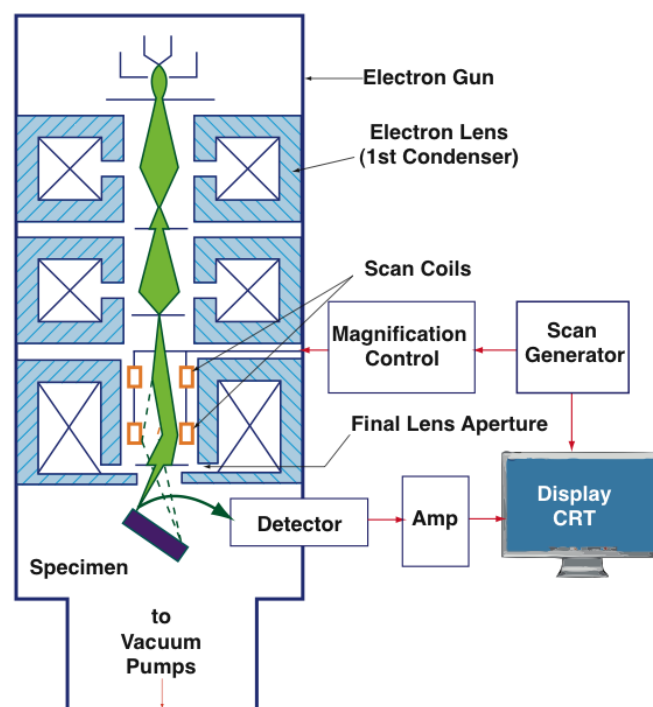


Figure 3.12. Schematically representation the main components of SEM column system

The SEM has a large depth of field about 30 mm, which allows a large amount of the sample to be in focus at the same time and produce an image that is a good representation of the three-dimensional sample. In addition, the combination of higher magnification,

large depth of field, greater resolution, compositional and crystallographic information makes the SEM one of the most highly used in lab searches area and industry. A SEM may be equipped with an EDX analysis system to enable it to perform compositional analysis on specimens. EDX analysis is useful in identifying materials and contaminants, as well as estimating their relative concentrations on the surface of the specimen (Stadtlander 2007).

#### **3.2.4. EDX**

Energy-dispersive X-ray spectroscopy (EDX) is a type of spectroscopy used by SEM to provide information on the chemical composition of the sample being examined in the SEM (Figure 3.13). Compared to other spectroscopic techniques used for the same purpose, it is quite advantageous. In EDX, when the electron beam transmitted to the sample interacts with the atoms of the sample, the energy is around 10-20 keV, causing X-ray photons to spread through the sample. Detection of these emitted photons is carried out by means of an energy separation spectrometer. EDX is based on the principle that the produced x-rays are measured as a function of the energy, and the chemical composition of the sample to be examined is determined according to the properties of the x-rays emitted from the sample. The portion of the sample to be analyzed may be the entire sample, a region, or any point. Thus, chemical analysis of any desired region during image acquisition can be performed. The energy of x-ray photons generated by sending an electron beam depends on the characteristics of the sample under investigation. As the emitted electrons form x-rays in the inner regions rather than the sample surface, EDX does not give information about the surface properties. In addition, Also, it is not very useful to use it in EDX analyzes because the X-ray intensity of elements with low atomic number is low. The fact that the EDX analysis can be performed at the same time as the acquisition of the SEM image, and the analysis without making the sample dissolve by any means, is a significant advantage of EDX (URL-3-4 2016). The EDX system used in our studies (JEOL JSM-6510) shown in Figure 3.13



Figure 3.13. The EDX and SEM system we use in our studies (JEOL JSM-6510)

### 3.2.5. XRD

The X-ray diffraction method is widely used in the determination of crystal structures. XRD devices have improved significantly after the Fourier Transform revolution. Sharp wide angle, short time and suitable output devices were analyzing each angle individually prior to offering a collective value. The ability to collect fingerprint sensitive data in crystal structures makes XRD very useful and reliable. The XRD Crystal is a technique that can determine the distance between atomic planes. The working principle is based on the collection of scatter and diffraction data by sending and scanning the x-ray to the sample to be analyzed. The X-rays are sent to a crystal plane and reflected by the crystal plane of the atoms, which is an X-ray diffraction phenomenon. This actual reflection is different from the reflection of the light from a mirror plane. Diffraction is not a superficial phenomenon. In other words, incoming x-rays reach the plane of the atoms beneath the crystal surface.

Wavelength fixed X-rays are used in XRD studies. To obtain these x-rays, electrons emitted by heating a filament, such as tungsten, is accelerated in the field and accelerated to an electron beam which is energized with high energy. These electrons reach the anodic electron shells (Skoog et al., 1998). If the electron beam collides with an electron in the shell near the core, the electron is removed from its position and the atom becomes

unstable due to electron loss. When If the vacant electron fills an electron in the higher energy crust shell, an energy difference occurs due to this electron transition, and this energy difference is spread as a photon of X-rays.

A way in which the rays reflected by the atomic planes collide with the X-ray beam at a certain angle, known as the Bragg angle, which is equal to the exact multiple of the wavelength ( $\lambda$ ), the rays will have the same phase and the diffraction will occur come to a point. It is shown in Figure (3.15), to obtain the diffraction peak; It is necessary to have a relation between the angle of attack ( $\theta$ ) of the x-rays to the atomic planes, the distance ( $d$ ) between the atomic planes and the wavelength  $\lambda$  of the incoming X-rays, The difference between the lengths of the paths that X-rays take it (Erdoğan 2009).

X-ray diffraction is a powerful tool to study the crystal structure of semiconductors. XRD gives information about crystalline phase, quality, orientation, composition, lattice parameters, defects, stress, and strain of samples. Every crystalline solid has its unique characteristic X-ray diffraction pattern, which is identified by this unique “fingerprint”. Crystals are regular arrays of atoms and they are arranged in a way that a series of parallel planes separated from one another by a distance  $d$ . Figure 3.14 shows the detail of the process of x-ray diffraction. If an x-ray beam with a wavelength strikes the sample with an incident angle then the scattered ray is determined by Bragg’s law ( $n = 2d\sin$ ). Where  $n$  is an integer, is the wavelength of the beam,  $d$  is the spacing between diffracting planes, and is the incident angle of the beam. The set of  $d$ -spacing in a typical x-ray scan provides a unique characteristic of the samples in question (Amin and Willander2012).

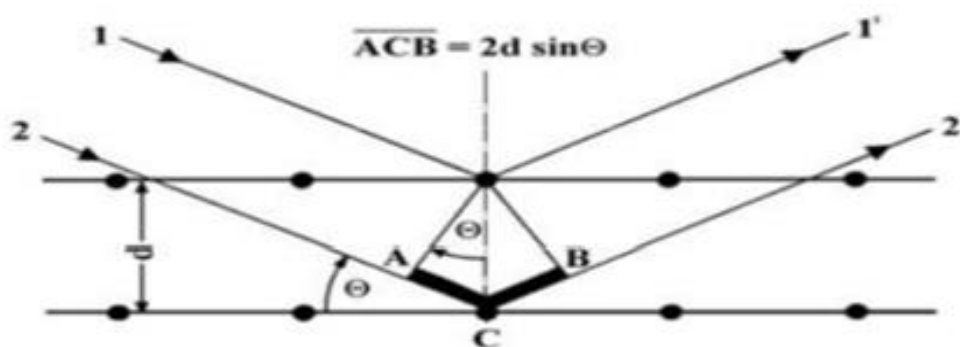


Figure 3.14. Schematic diagram of Bragg's reflection from lattice planes in a crystalline structure with development of x-ray diffraction

$$ACB = AC + CB \quad (3.4)$$

$$\sin\theta = AC / d = CB / d \quad (3.5)$$

$$AC = CB = d \sin\theta \quad (3.6)$$

The difference between the lengths of the paths of the X-rays is given by Equation 3.7 below.

$$AC + CB = 2d \sin\theta \quad (3.7)$$

$$ACB = 2d \sin\theta \quad (3.8)$$

In order for the diffraction to be possible, this path difference must be equal to the multiple of  $\lambda$  or  $n\lambda$ . Thus Equation 3.8 can be written (Erdoğan 2009).

$$ACB = n\lambda \quad (3.9)$$

$$2d \sin\theta = n\lambda \quad (3.10)$$

The XRD device used in our studies is shown in Figure 3.16.



Figure 3.15. The XRD device (RigakuUltima IV)



### 3.2.6. Photoelectrochemical System

The photoelectrocatalytic performances of these oxides formed on ITO coated glass electrodes were measured under sunlight, which is represented by a three-electrode system (Figure 3.19). The photoelectrochemical measurements were recorded under a beam of AM 1.5G using a Solar Light-16S-002 brand solar simulator with a 150 W xenon arc lamp. The photocurrent-potential, and photocurrent-time curves were measured using linear sweep voltammetry and chronoamperometry techniques, respectively.

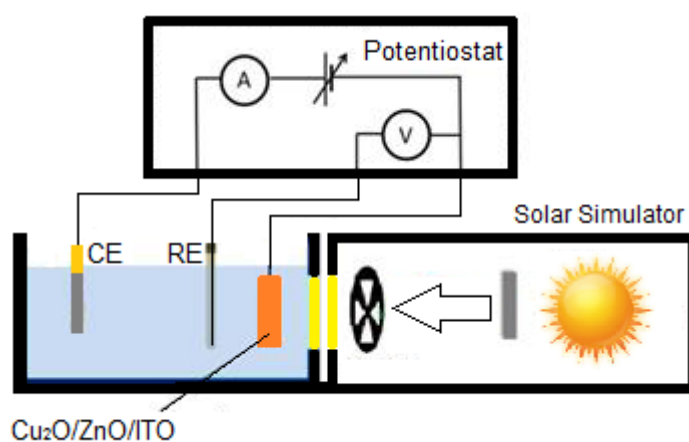


Figure 3.16. Schematic representation of the instrument used for photoelectrochemical measurements

## 4. FINDINGS AND DISCUSSION

### 4.1. Electrochemical Studies

The general experimental strategy employed in this thesis study was the atom-by-atom growth of ZnO thin films and Cu<sub>2</sub>O nanocubes using the UPD of each element. In principle, UPD, the electrochemical deposition of a metal onto a substrate at potentials more positive than the Nernst potential, is usually restricted to the formation of one atomic layer of the deposited metal. Therefore, in order to deposit an atom at a time, very small amounts of dissolved Zn<sup>2+</sup> and Cu<sup>2+</sup> species are needed in the solution phase for deposition at UPD. The UPD potentials for both Zn and Cu were determined by cyclic voltammetric measurements. In order to determine a deposition potential of the ZnO from the solution, the cyclic voltammetric measurements of zinc were recorded at the UPD region in the aqueous medium. The results showed that the bulk zinc deposition does not occur until  $-700$  mV. If the potential of the working electrode is kept constant at a more positive potential than  $-700$  mV, Zn and O are supposed to deposit underpotentially at the electrode surface. These electrodeposited Zn and O react to form the ZnO semiconductor on ITO coated glass surface. ZnO films deposited on ITO coated glass surface for 1 h. Cu<sub>2</sub>O nanocubes electrodeposited on ZnO coated surface at different deposition times (1, 3, 5, 10 and 15 minutes).

In order to determine a deposition potential of the Cu<sub>2</sub>O from the solution, the cyclic voltammetric measurements of copper were also recorded at the UPD region in the aqueous medium. The results showed that the bulk copper deposition does not occur until  $-200$  mV. If the potential of the ZnO coated working electrode is kept constant at a more positive potential than  $-200$  mV, Cu and O are supposed to deposit underpotentially at the electrode surface. These electrodeposited Cu and O react to form the Cu<sub>2</sub>O semiconductor on ZnO coated surface. The amount of electrodeposited ZnO and Cu<sub>2</sub>O will depend on the deposition time. Thus, electrodepositions of Cu<sub>2</sub>O nanocubes with

various dimensions on ZnO coated surface could be achieved by this method using different deposition times.

#### 4.2. XRD Studies

Figure 4.1 shows the XRD patterns of the electrodeposited ZnO films on ITO coated glass. The XRD diffractogram of ZnO electrodeposited for 1 h consists of a strong diffraction peak at  $36.5^\circ$  ( $2\theta$  scale) arising from (1 0 1) reflections from ZnO. The weaker diffractions at  $32.1^\circ$ ,  $34.5^\circ$ ,  $47.8^\circ$ ,  $57.2^\circ$ ,  $63.1^\circ$ , and  $68.5^\circ$  corresponds to (1 0 0), (0 0 2), (1 0 2), (1 1 0), (1 0 3), and (1 1 2) reflections of ZnO. The other peaks belong to ITO coated glass which belongs to working electrode in this study.

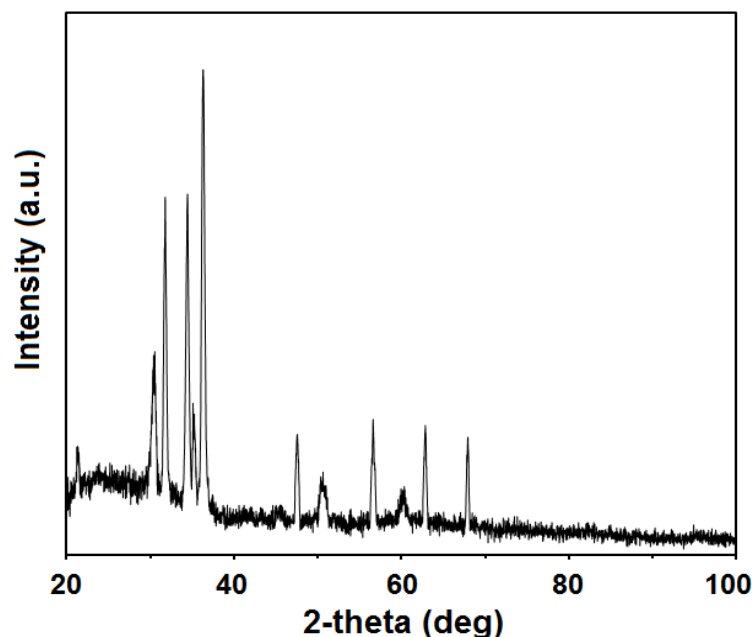


Figure 4.1. The XRD diffractogram of ZnO films electrodeposited onto ITO coated glass surface

Figure 4.2 and 4.3 are XRD diffractograms of ZnO films decorated with  $\text{Cu}_2\text{O}$  nanocubes electrodeposited for 1 and 3 min, respectively. All the peaks belong to ZnO and ITO coated glass. No peaks belong to  $\text{Cu}_2\text{O}$  was detected in XRD patterns. The single-phase ZnO was observed for ZnO films decorated with  $\text{Cu}_2\text{O}$  nanocubes electrodeposited for 1 and 3 min.

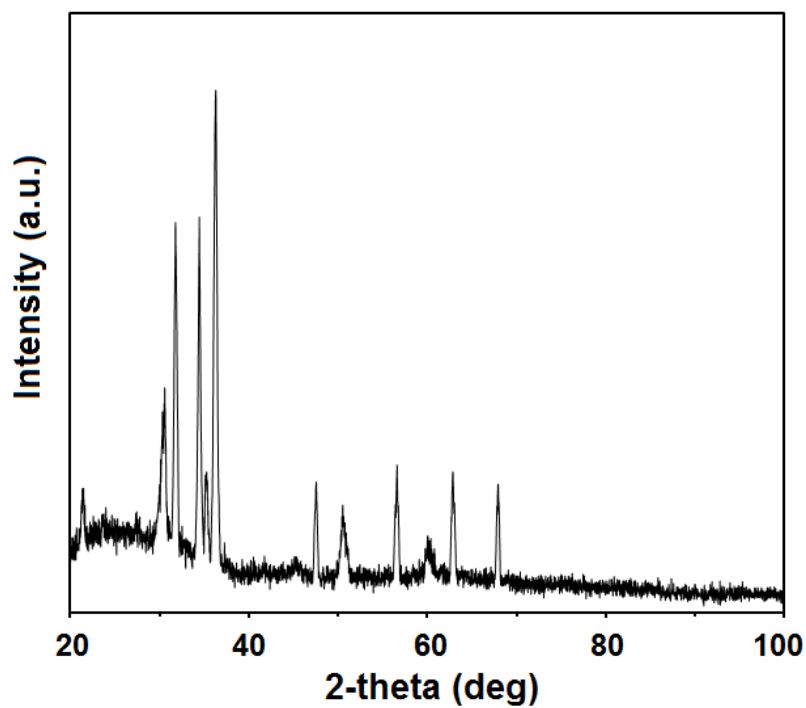


Figure 4.2. The XRD diffractogram of ZnO films decorated with Cu<sub>2</sub>O nanocubes electrodeposited for 1 min

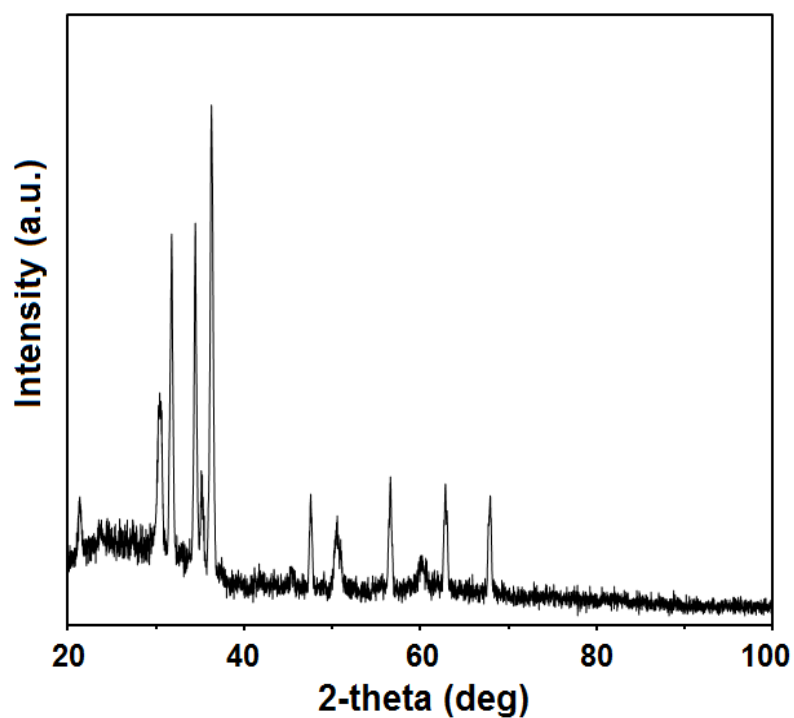


Figure 4.3. The XRD diffractogram of ZnO films decorated with Cu<sub>2</sub>O nanocubes electrodeposited for 3 min

When the deposition time increased to 5 min (Figure 4.4), the weak peaks appeared at around  $36.6^\circ$ ,  $42.5^\circ$ ,  $61.7^\circ$  and  $73.9^\circ$ , corresponding to the (1 1 1), (2 0 0), (2 2 0) and (3 1 1) peaks of  $\text{Cu}_2\text{O}$ .

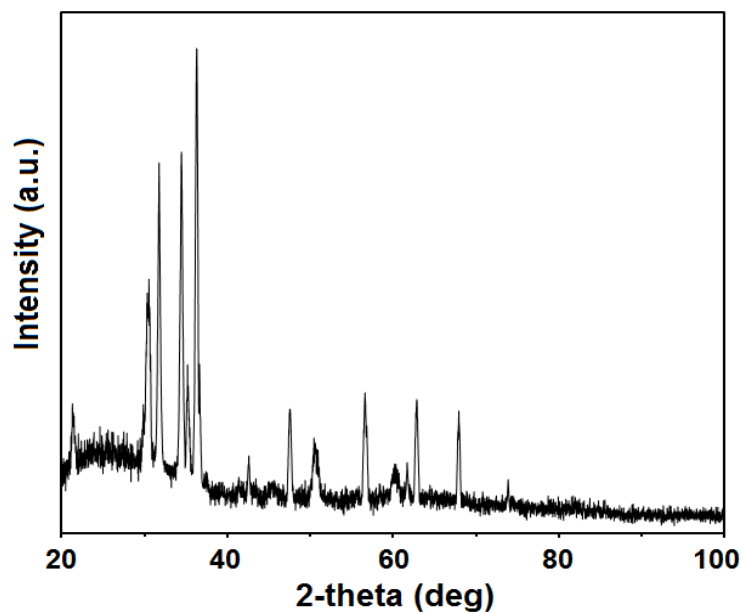


Figure 4.4. The XRD diffractogram of ZnO films decorated with  $\text{Cu}_2\text{O}$  nanocubes electrodeposited for 5 min

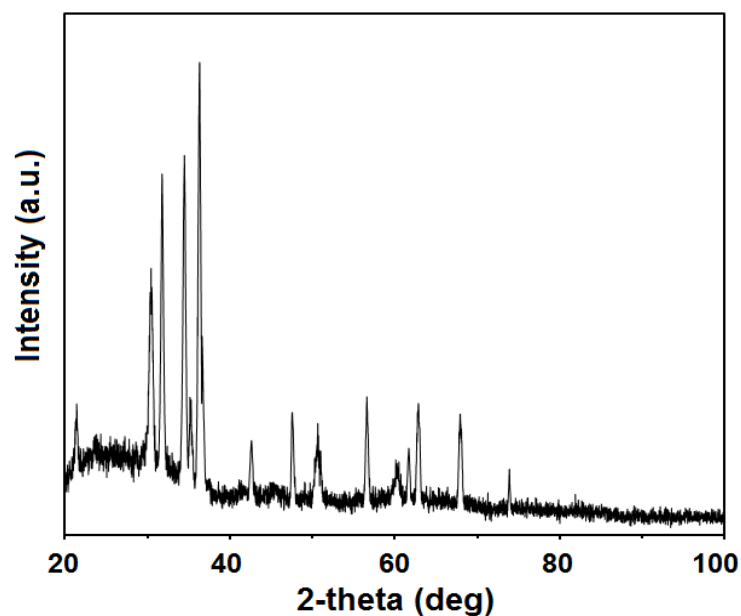


Figure 4.5. The XRD diffractogram of ZnO films decorated with  $\text{Cu}_2\text{O}$  nanocubes electrodeposited for 10 min

It was revealed that a secondary phase of  $\text{Cu}_2\text{O}$  evolved when  $\text{Cu}_2\text{O}$  at more high deposition times than 5 min was doped into ZnO films. As the deposition time increases, the intensity of  $\text{Cu}_2\text{O}$  reflections increases (Figure 4.5 and 4.6).

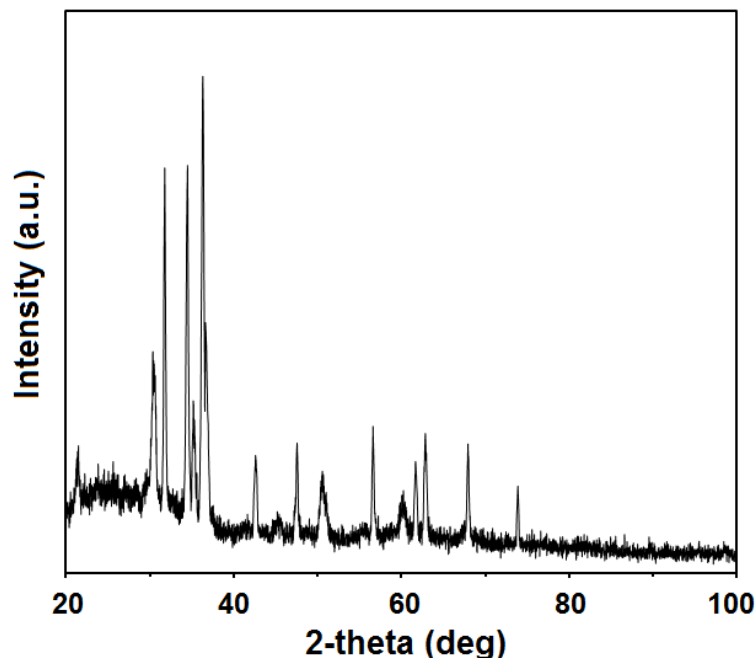


Figure 4.6. The XRD diffractogram of ZnO films decorated with  $\text{Cu}_2\text{O}$  nanocubes electrodeposited for 15 min

### 4.3. SEM and EDX Studies

Figure 4.7 shows SEM image of ITO coated glass surface which belongs to working electrode in this study. Figure 4.8 shows a SEM image obtained after electrodeposition of ZnO on ITO coated glass for 1 h. The ITO coated glass surface is completely covered with ZnO.

Figure 4.9 and 4.10 are SEM images of ZnO films decorated with  $\text{Cu}_2\text{O}$  nanocubes electrodeposited for 1 and 3 min, respectively. Figure 4.9 shows the SEM image of the initial stages of the nucleation and growth of  $\text{Cu}_2\text{O}$  electrodeposited on ITO coated glass for 1 min. Evenly distributed nano-seeds of approximately the same size are observed on the surface of the ZnO coated electrode. Most nanocubes have a uniform shape. The average sizes of  $\text{Cu}_2\text{O}$  nanocubes observed for 1 min were about 75 nm in diameter.

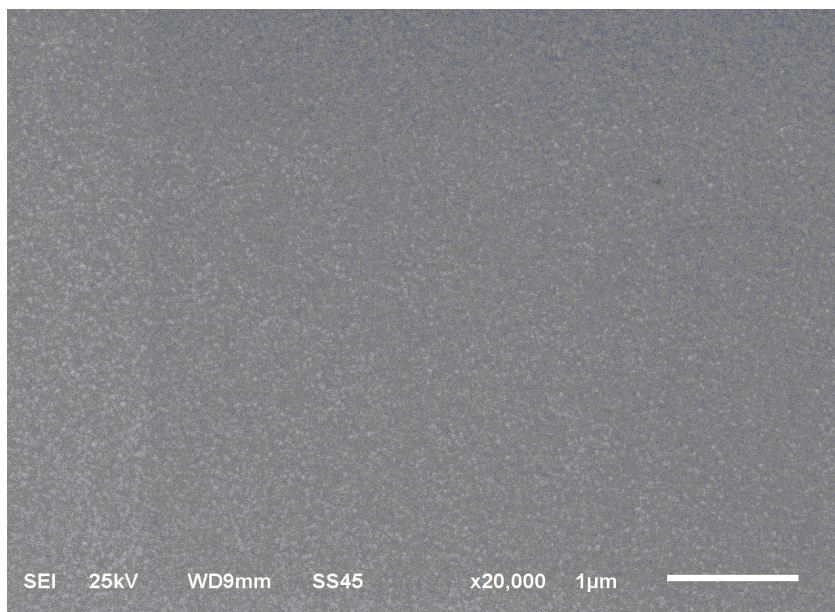


Figure 4.7. SEM image of ITO coated glass surface

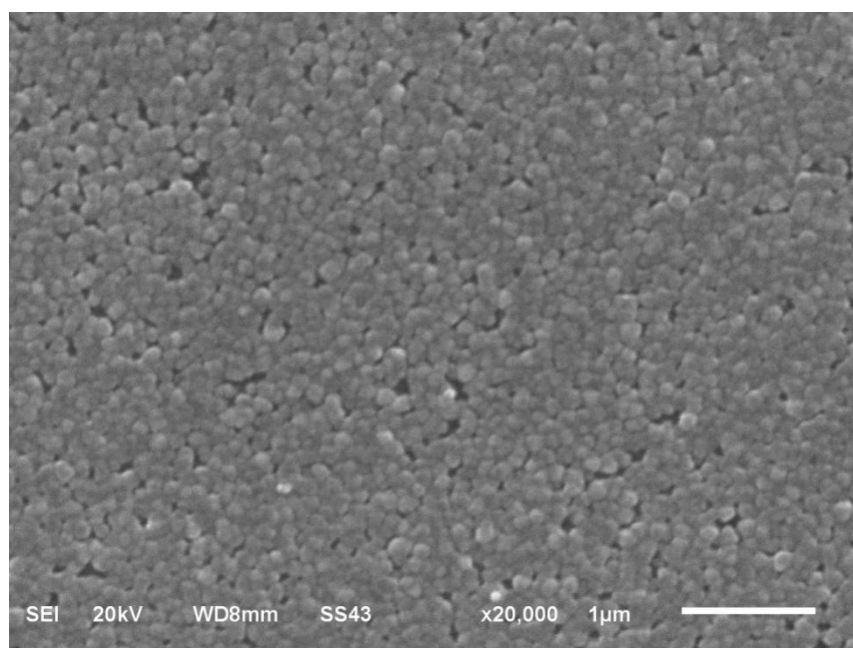


Figure 4.8. SEM image of ZnO films electrodeposited onto ITO coated glass surface

As the electrodeposition time increases to 3 min, nanocubes diameters increase and the other crystals form at the surface (Figure 4.10). The average sizes of  $\text{Cu}_2\text{O}$  nanocubes observed for 3 min were about 100 nm in diameter.

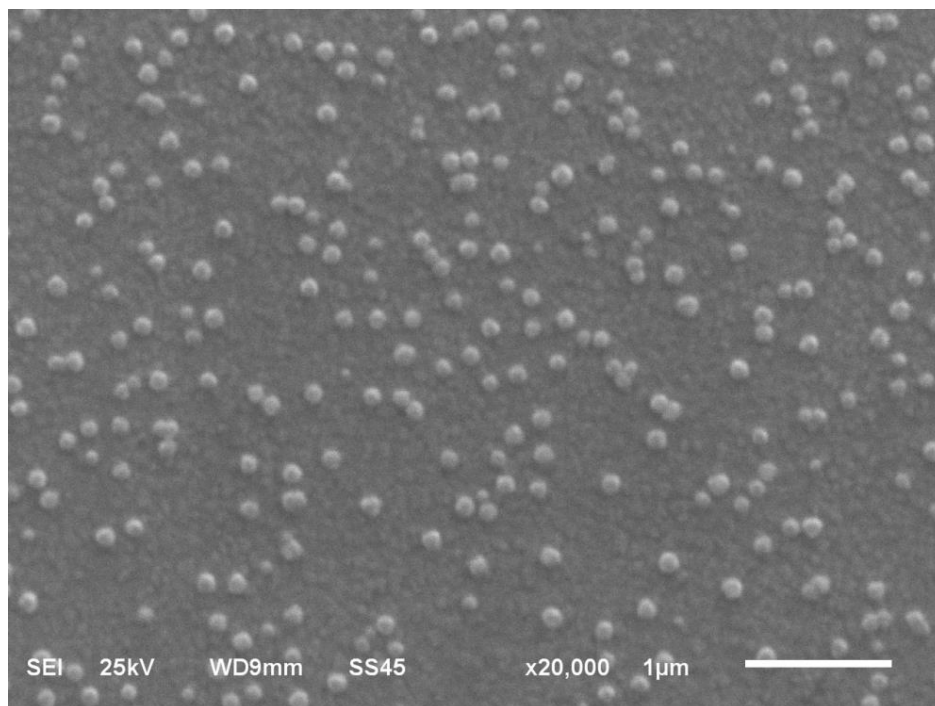


Figure 4.9. SEM image of ZnO films decorated with  $\text{Cu}_2\text{O}$  nanocubes electrodeposited for 1 min

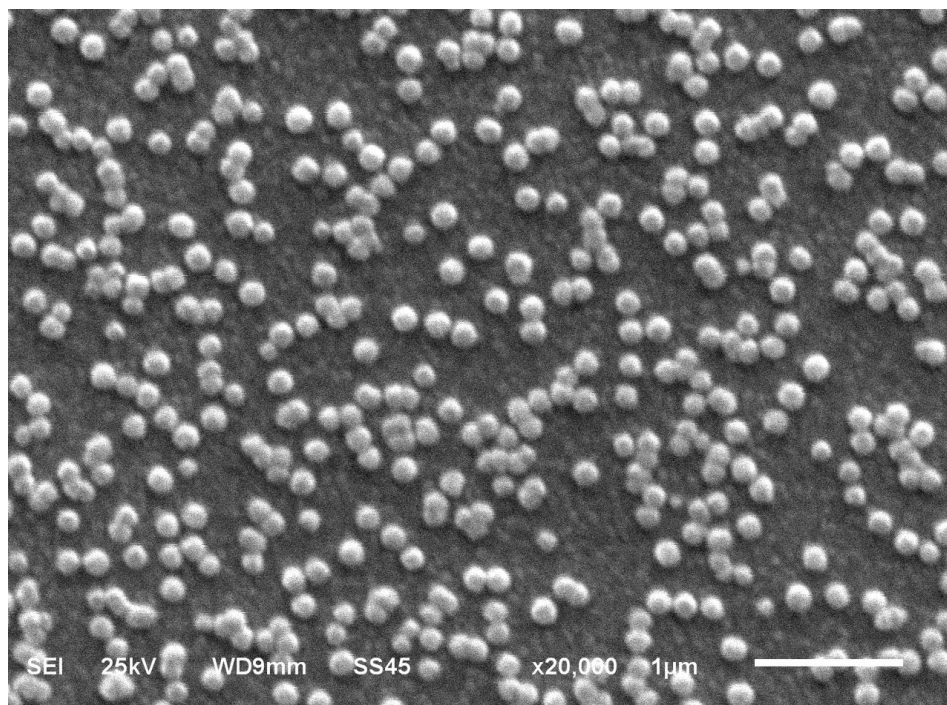


Figure 4.10. SEM image of ZnO films decorated with  $\text{Cu}_2\text{O}$  nanocubes electrodeposited for 3 min



Figure 4.11 and 4.12 show two SEM images obtained after electrodeposition of  $\text{Cu}_2\text{O}$  for 5 and 10 min, respectively. The average sizes of  $\text{Cu}_2\text{O}$  nanocubes observed for 5 and 10 min were about 150 and 200 nm in diameter, respectively.

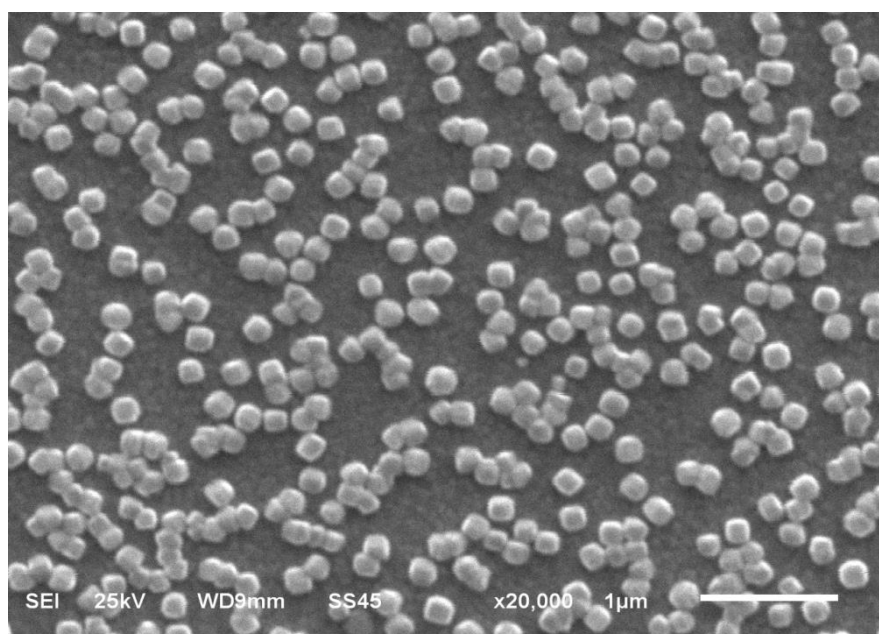


Figure 4.11. SEM image of ZnO films decorated with  $\text{Cu}_2\text{O}$  nanocubes electrodeposited for 5 min

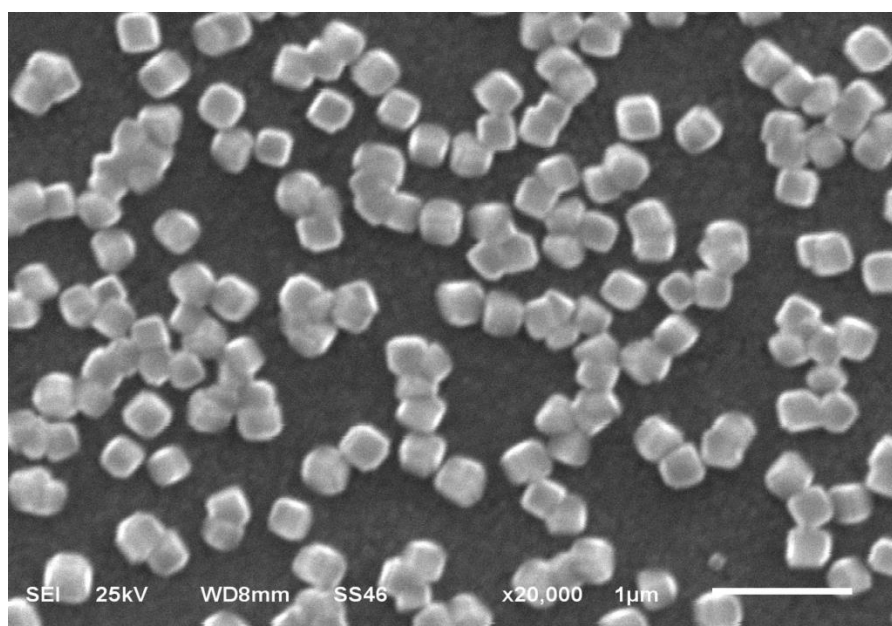


Figure 4.12. SEM image of ZnO films decorated with  $\text{Cu}_2\text{O}$  nanocubes electrodeposited for 10 min

Figure 4.13 shows two SEM image obtained after electrodeposition of  $\text{Cu}_2\text{O}$  for 15 min. The average size of  $\text{Cu}_2\text{O}$  nanocubes were about 250 nm in diameter.

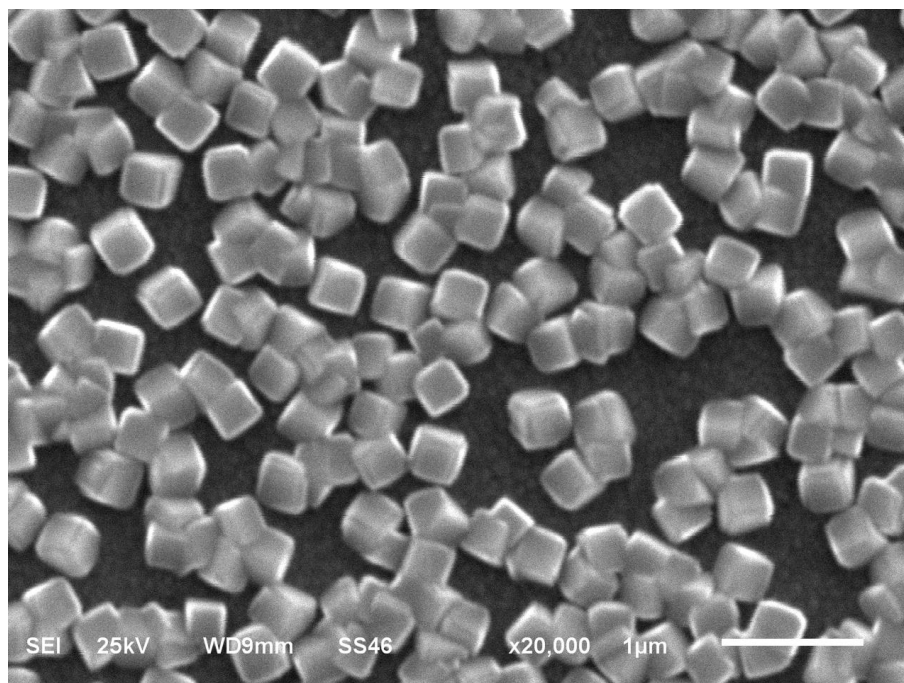


Figure 4.13. SEM image of ZnO films decorated with  $\text{Cu}_2\text{O}$  nanocubes electrodeposited for 15 min

The elemental compositions of the electrodeposited ZnO films and  $\text{Cu}_2\text{O}$  cubes were determined by the EDX. The absence of any other peaks indicates that the ZnO and  $\text{Cu}_2\text{O}$  are homogeneous in composition and formed from Zn-O and Cu-O. EDX analyses of different regions gave the same results. For the ZnO films decorated with  $\text{Cu}_2\text{O}$  nanocubes, the quantitative atomic ratios of Zn/O and Cu/O are close to 1/1 and 1/2 stoichiometry, respectively.

#### 4.4. Absorbance and Band Gap Studies

Figure 4.14 shows the optical absorption spectra of ZnO films electrodeposited onto ITO coated glass surface in the range of 300–800 nm. Only an absorption in the UV-Vis region can be observed. The absorption edge measured for the films is 365 nm. The fundamental absorption edge at 365nm corresponds to bulk ZnO.

Absorbance spectrum of ZnO films decorated with Cu<sub>2</sub>O nanocubes electrodeposited for 1 min is shown in Figure 4.15. In here, two absorption bands in the UV-Vis region observed. The absorption edge measured for the electrodes are 368 and 540 nm. The fundamental absorption edges at 368 and 540 nm correspond to ZnO and Cu<sub>2</sub>O, respectively.

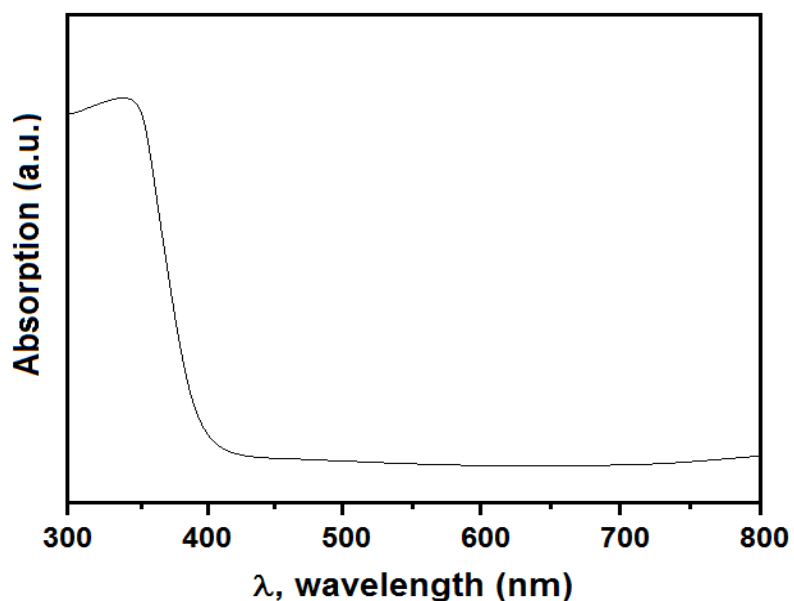


Figure 4.14. Absorbance spectrum of ZnO films electrodeposited onto ITO coated glass surface

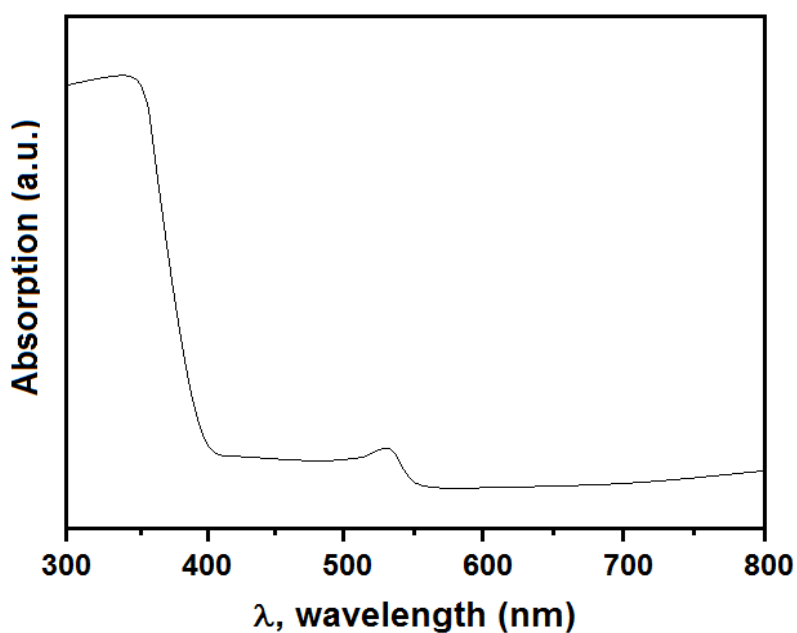


Figure 4.15. Absorbance spectrum of ZnO films decorated with Cu<sub>2</sub>O nanocubes electrodeposited for 1 min

Absorbance spectra of ZnO films decorated with Cu<sub>2</sub>O nanocubes electrodeposited for 3 and 5 min is shown in Figure 4.16 and 4.17. In Figure 4.16, the absorption edge measured for the electrodes are 370 and 555 nm. In Figure 4.17, the absorption edge measured for the electrodes are 373 and 570 nm. These fundamental absorption edges correspond to ZnO and Cu<sub>2</sub>O.

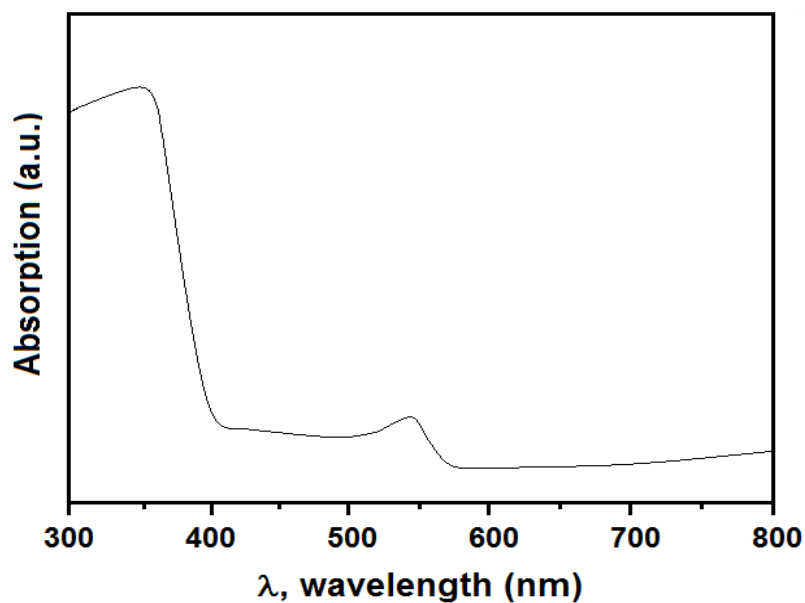


Figure 4.16. Absorbance spectrum of ZnO films decorated with Cu<sub>2</sub>O nanocubes electrodeposited for 3 min

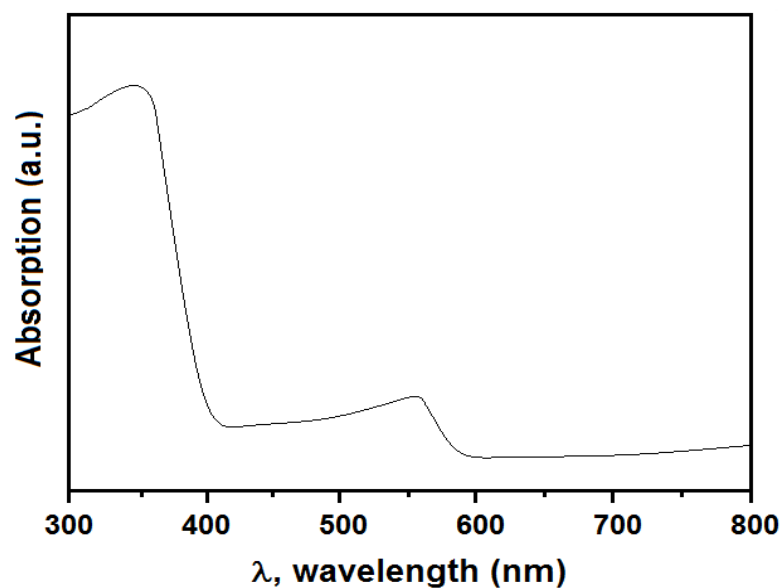


Figure 4.17. Absorbance spectrum of ZnO films decorated with Cu<sub>2</sub>O nanocubes electrodeposited for 5 min

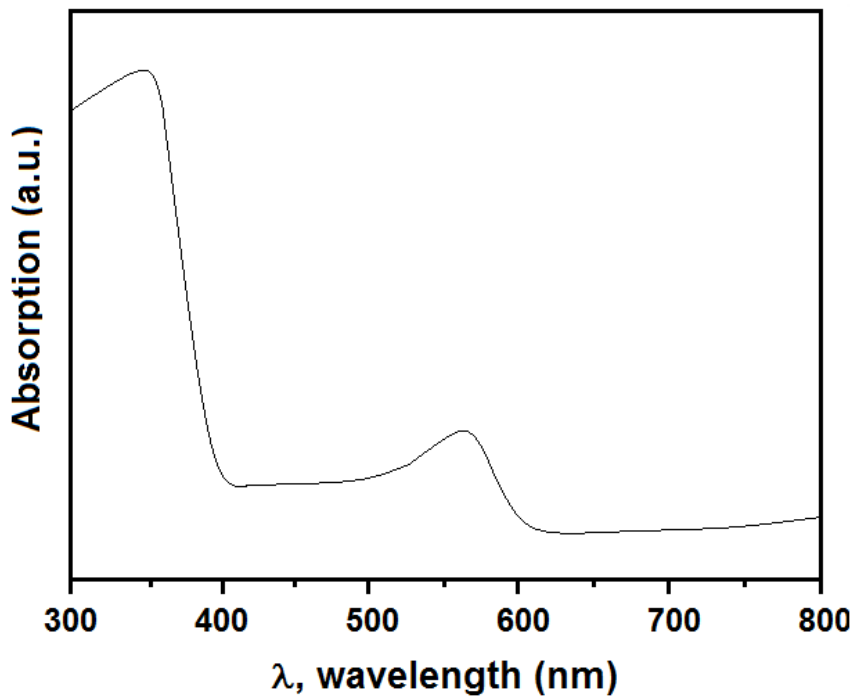


Figure 4.18. Absorbance spectrum of ZnO films decorated with Cu<sub>2</sub>O nanocubes electrodeposited for 10 min

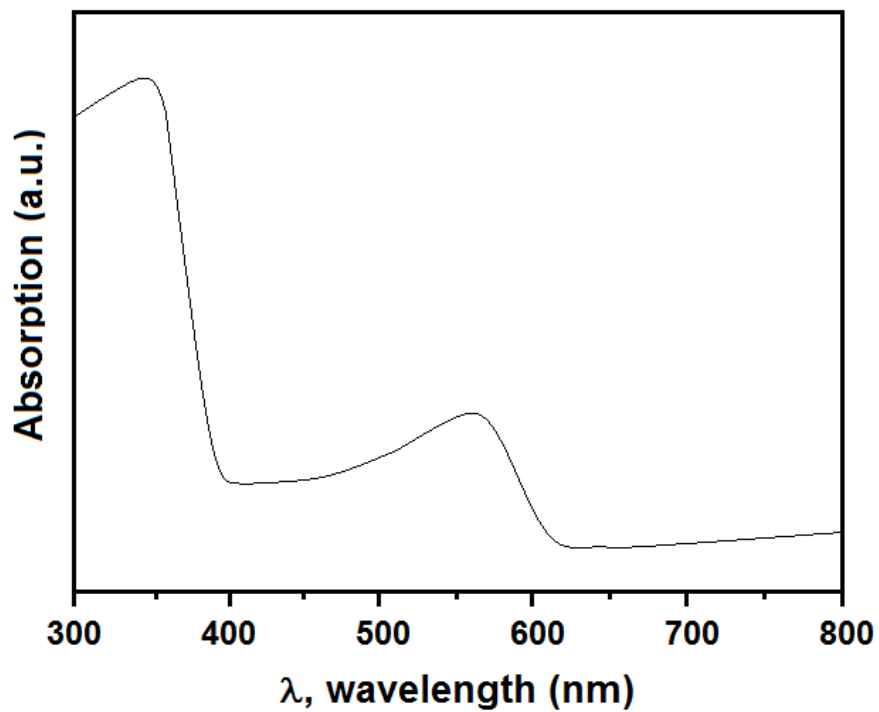


Figure 4.19. Absorbance spectrum of ZnO films decorated with Cu<sub>2</sub>O nanocubes electrodeposited for 15 min

Absorbance spectra of ZnO films decorated with Cu<sub>2</sub>O nanocubes electrodeposited for 10 and 15 min is shown in Figure 4.18 and 4.19. In Figure 4.18, the absorption edge measured for the electrodes are 375 and 580 nm. In Figure 4.17, the absorption edge measured for the electrodes are 380 and 590 nm. These fundamental absorption edges correspond to ZnO and Cu<sub>2</sub>O.

For semiconductors, the widely used method of plotting  $(\alpha hv)^2$  versus the energy  $hv$  is adopted to determine the band gap of the semiconductors. The  $E_g$  can thus be estimated from a plot of  $(\alpha hv)^2$  versus the photon energy  $hv$ . The band gap of ZnO film electrodeposited onto ITO coated glass was found to be  $E_g = 3.40$  eV. The band gaps of ZnO in ZnO films decorated with Cu<sub>2</sub>O nanocubes were found to be  $E_g = 3.37, 3.35, 3.32, 3.30$  and  $3.26$  eV for 1, 3, 5, 10 and 15 min, respectively. The band gaps of Cu<sub>2</sub>O in ZnO films decorated with Cu<sub>2</sub>O nanocubes were found to be  $E_g = 2.30, 2.23, 2.18, 2.14$  and  $2.10$  for 1, 3, 5, 10 and 15 min, respectively.

#### 4.5. PEC Studies

Figure 4.20 exhibits linear sweep voltammograms of ZnO films electrodeposited onto ITO coated glass surface in dark and light. This voltammogram show a photoanodic behavior due to the n-type nature of the ZnO semiconductors.

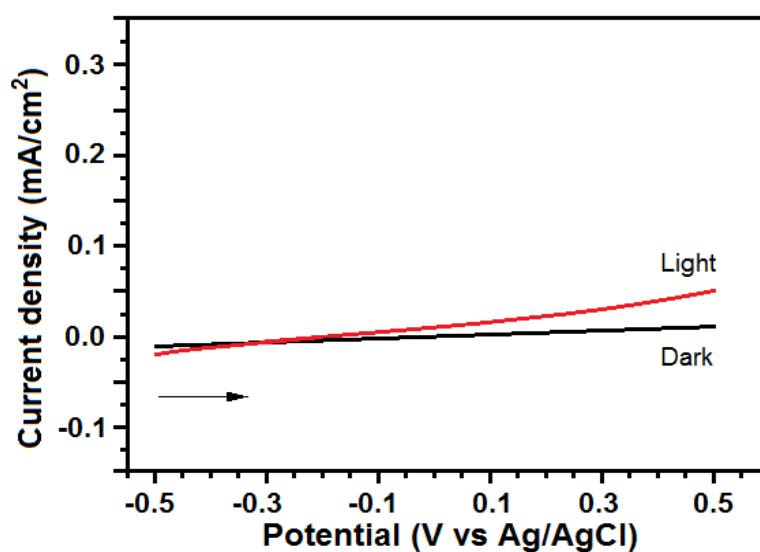


Figure 4.20. Linear sweep voltammograms of ZnO films electrodeposited onto ITO coated glass surface in 0.1 M Na<sub>2</sub>SO<sub>4</sub>

Figure 4.21-25 shows the effect of  $\text{Cu}_2\text{O}$  nanocubes growth time on the light and dark currents of semiconductor films. Figure 4.21 and 22 exhibit linear sweep voltammograms of ZnO films decorated with  $\text{Cu}_2\text{O}$  nanocubes for 1 and 3 min, respectively. The photocurrents increase with longer deposition time. The ZnO films doped with  $\text{Cu}_2\text{O}$  nanocubes for 3 min exhibit the highest photocurrents between the investigated all semiconductor films.

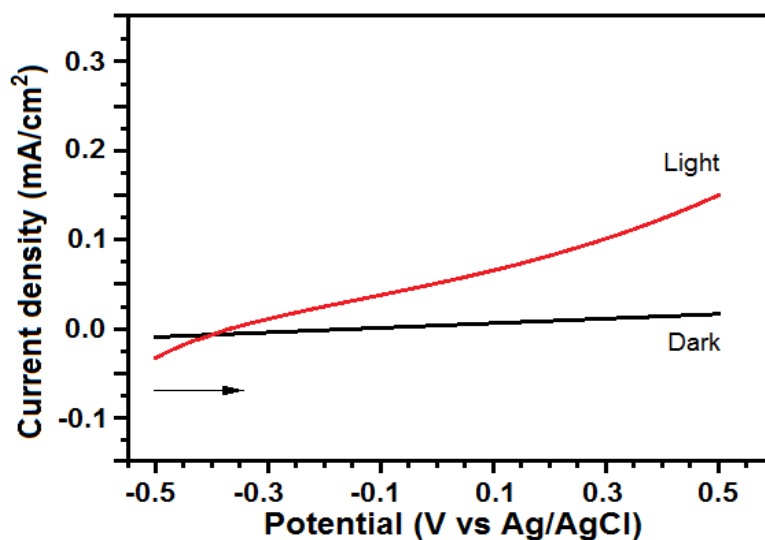


Figure 4.21. Linear sweep voltammograms of ZnO films decorated with  $\text{Cu}_2\text{O}$  nanocubes electrodeposited for 1 min in 0.1 M  $\text{Na}_2\text{SO}_4$

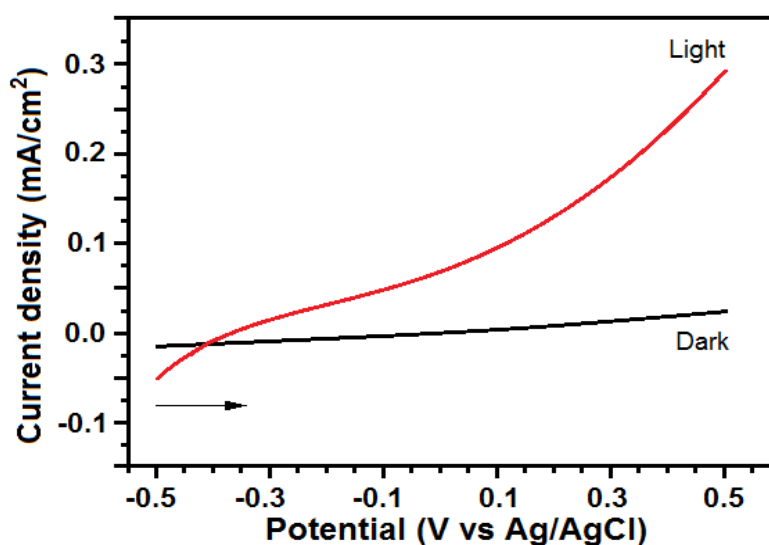


Figure 4.22. Linear sweep voltammograms of ZnO films decorated with  $\text{Cu}_2\text{O}$  nanocubes electrodeposited for 3 min in 0.1 M  $\text{Na}_2\text{SO}_4$

Despite the higher surface area of ZnO films doped with Cu<sub>2</sub>O nanocubes for higher deposition times, they show lower photocurrents than the ZnO films doped with Cu<sub>2</sub>O nanocubes for 3 min (Figure 4.23-25). This may be due to the increased bending of ZnO films doped with Cu<sub>2</sub>O nanocubes for higher deposition times, which may reduce the effective area for surface reactions leading to lower photocurrents.

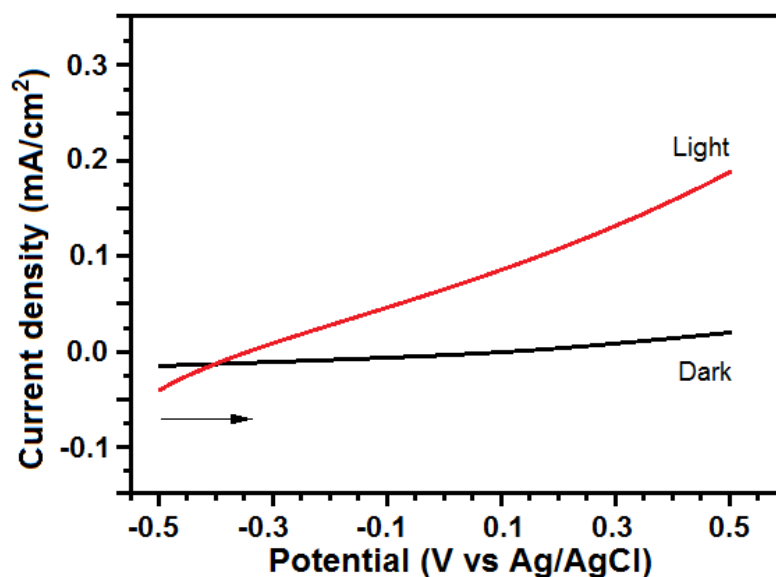


Figure 4.23. Linear sweep voltammograms of ZnO films decorated with Cu<sub>2</sub>O nanocubes electrodeposited for 5 min in 0.1 M Na<sub>2</sub>SO<sub>4</sub>

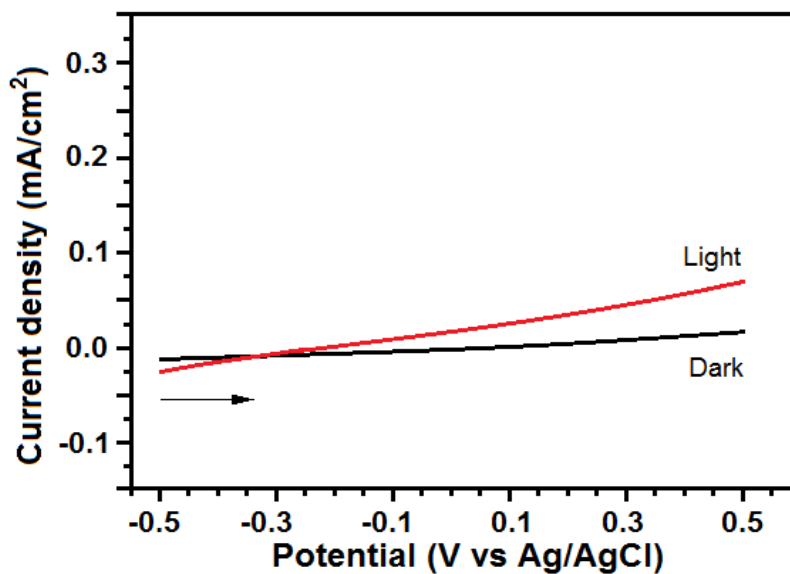


Figure 4.24. Linear sweep voltammograms of ZnO films decorated with Cu<sub>2</sub>O nanocubes electrodeposited for 10 min in 0.1 M Na<sub>2</sub>SO<sub>4</sub>



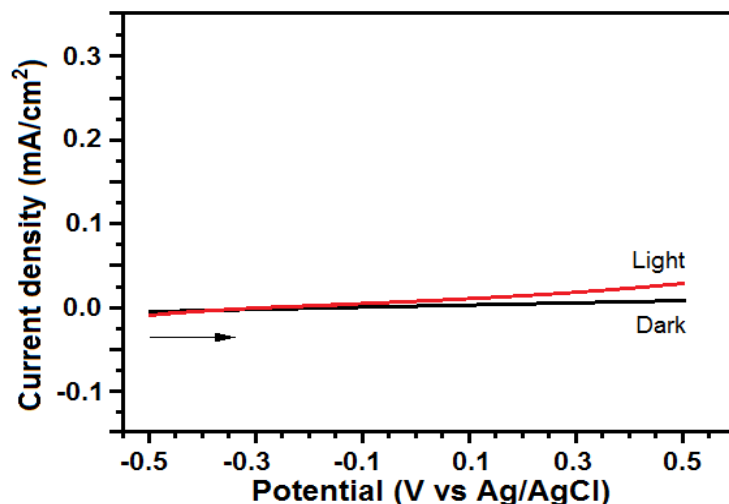


Figure 4.25. Linear sweep voltammograms of ZnO films decorated with Cu<sub>2</sub>O nanocubes electrodeposited for 15 min in 0.1 M Na<sub>2</sub>SO<sub>4</sub>

Figure 4.26 illustrates the transient current density under sun light for the corresponding single phase ZnO and ZnO films decorated with Cu<sub>2</sub>O nanocubes. Herein, the effect of Cu<sub>2</sub>O electrodeposition time on the photocurrents of photoactive films is exhibited. The trends for different Cu<sub>2</sub>O growth times in the current density (Figure 4.26) confirm the observed trends in Figure 4.21-25. As shown in Figure 4.26, ZnO films decorated with Cu<sub>2</sub>O nanocubes exhibit good switching behavior for different Cu<sub>2</sub>O growth times.

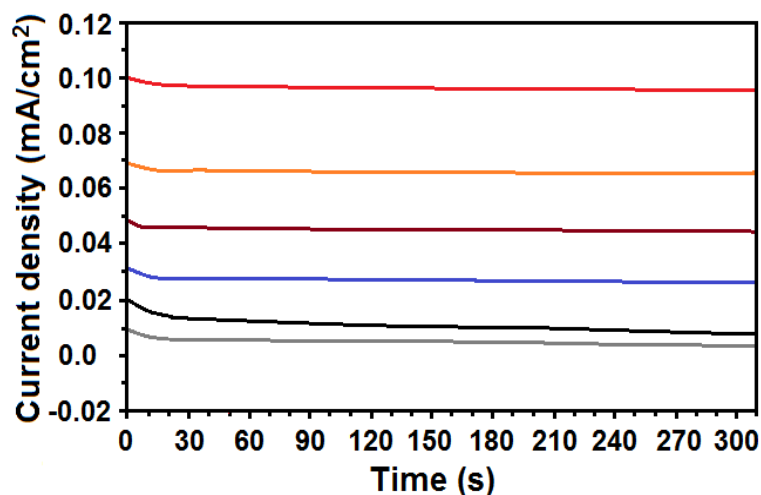


Figure 4.26. Photocurrent responses of the films under light illumination in 0.1 M Na<sub>2</sub>SO<sub>4</sub>. Black line show photocurrent density of ZnO films electrodeposited onto ITO coated glass. Current density of ZnO films decorated with different Cu<sub>2</sub>O nanocubes (brown line, 1 min; red line, 3 min; orange line, 5 min; blue line, 10 min; grey line, 15 min)

## 5. RESULTS AND RECOMMENDATIONS

This work reported on a systematic study of the influence of Cu<sub>2</sub>O nanocubes decorating on the structural, optical and photoelectrochemical characteristics of ZnO films. ZnO and ZnO/Cu<sub>2</sub>O semiconductors were prepared by practical electrochemical method, based on the underpotential deposition (UPD). The general experimental strategy employed in this thesis study was the atom-by-atom growth of ZnO thin films and Cu<sub>2</sub>O nanocubes using the UPD of each element. The UPD potentials for both Zn and Cu were determined by cyclic voltammetric measurements. ZnO films deposited on ITO coated glass surface for 1 h. Cu<sub>2</sub>O nanocubes electrodeposited on ZnO coated surface at different deposition times (1, 3, 5, 10 and 15 minutes). Thus, electrodepositions of Cu<sub>2</sub>O nanocubes with various dimensions on ZnO coated surface could be achieved by this method using different deposition times.

The XRD diffractogram of ZnO electrodeposited for 1 h consists of a strong diffraction peak at 36.5° (2θ scale) arising from (1 0 1) reflections from ZnO. For XRD diffractograms of ZnO films decorated with Cu<sub>2</sub>O nanocubes electrodeposited for 1 and 3 min, all the peaks belong to ZnO and ITO coated glass. No peaks belong to Cu<sub>2</sub>O was detected in XRD patterns. The single-phase ZnO was observed for ZnO films decorated with Cu<sub>2</sub>O nanocubes electrodeposited for 1 and 3 min. When the deposition time increased to 5 min, the weak peaks appeared the peaks corresponding to the diffractions of Cu<sub>2</sub>O. It was revealed that a secondary phase of Cu<sub>2</sub>O evolved when Cu<sub>2</sub>O at more high deposition times than 5 min was doped into ZnO films. As the deposition time increases, the intensity of Cu<sub>2</sub>O reflections increases.

SEM images were revealed that the ITO coated glass surface is completely covered with ZnO and Cu<sub>2</sub>O nano-seeds of approximately the same size are observed on the surface of the ZnO coated electrode. Most nanocubes have a uniform shape. The average sizes of Cu<sub>2</sub>O nanocubes observed for 1, 3, 5, 10 and 15 min were about 75, 100, 150, 200 and

250 nm in diameter. As the electrodeposition time increases, Cu<sub>2</sub>O nanocubes diameters increase and the other crystals form at the surface.

EDX analyses show that the absence of any other peaks indicates that the ZnO and Cu<sub>2</sub>O are homogeneous in composition and formed from Zn-O and Cu-O. EDX analyses of different regions gave the same results. For the ZnO films decorated with Cu<sub>2</sub>O nanocubes, the quantitative atomic ratios of Zn/O and Cu/O are close to 1/1 and 1/2 stoichiometry, respectively.

In the optical absorption spectra of ZnO films electrodeposited onto ITO coated glass surface, only an absorption in the UV-Vis region can be observed. The absorption edge measured for the films is 365 nm. The fundamental absorption edge at 365 nm corresponds to bulk ZnO.

Absorbance spectrums of ZnO films decorated with Cu<sub>2</sub>O nanocubes electrodeposited for 1, 3, 5, 10 and 15 min have the fundamental absorption edges correspond to ZnO and Cu<sub>2</sub>O. The band gap of ZnO film electrodeposited onto ITO coated glass was found to be  $E_g = 3.40$  eV. The band gaps of ZnO in ZnO films decorated with Cu<sub>2</sub>O nanocubes were found to be 3.37, 3.35, 3.32, 3.30 and 3.26 eV for 1, 3, 5, 10 and 15 min, respectively. The band gaps of Cu<sub>2</sub>O in ZnO films decorated with Cu<sub>2</sub>O nanocubes were found to be 2.30, 2.23, 2.18, 2.14 and 2.10 for 1, 3, 5, 10 and 15 min, respectively.

Linear sweep voltammograms show a photoanodic behavior due to the n-type nature of the semiconductors. The photocurrents increase with longer deposition time. The ZnO films doped with Cu<sub>2</sub>O nanocubes for 3 min exhibit the highest photocurrents between the investigated all semiconductor films. Despite the higher surface area of ZnO films doped with Cu<sub>2</sub>O nanocubes for higher deposition times, they show lower photocurrents than the ZnO films doped with Cu<sub>2</sub>O nanocubes for 3 min. The effect of Cu<sub>2</sub>O electrodeposition time on the photocurrents of photoactive films are exhibited. The trends for different Cu<sub>2</sub>O growth times in the current density confirm the observed trends in linear sweep voltammograms. ZnO films decorated with Cu<sub>2</sub>O nanocubes exhibit good switching behavior for different Cu<sub>2</sub>O growth times. This may be due to the increased bending of ZnO films doped with Cu<sub>2</sub>O nanocubes for higher deposition times, which

may reduce the effective area for surface reactions leading to lower photocurrents. ZnO films decorated with Cu<sub>2</sub>O nanocubes are suggested as a competitive candidate for advanced PEC detection, maybe for the extended field of PEC water splitting and other solar photovoltaic technologies.

## REFERENCES

Abd-ellah M, Thomas JP, Zhang L, Tong K (2016) Solar Energy Materials, Solar Cells Enhancement of solar cell performance of p-Cu<sub>2</sub>O/n-ZnO-nanotube and nanorod heterojunction devices. *Solar Energy Materials and Solar Cells* 152: 87–93

Alkoy EM, Kelly JM (2005) The structure and properties of copper oxide and copper aluminium oxide coating prepared by pulsed magnetron sputtering of powder targets

Amin G, Willander, PM (2012) ZnO and CuO Nanostructures Low Temperature Growth, Characterization, their Optoelectronic and Sensing Applications. Department of Science and Technology, Physics and Electronics

Barreca D, Carraro G, Gasparotto A, Maccato C, Cruz-Yusta M, Gomez-Camer JL, Sanchez L (2012) On the Performances of Cu<sub>x</sub>O-TiO<sub>2</sub> (x= 1,2) Nanomaterials As Innovative Anodes for Thin Film Lithium Batteries. *ACS applied materials interfaces* 4(7): 3610-3619

Bartlett PN, Baumberg JJ, Coyle S, Abdelsalam ME (2004) Optical properties of nanostructured metal films. *Faraday discussions* 125: 117-132

Bridgman PW, (1925) Certain Physical Properties of Single Crystals of Tungsten, Antimony, Bismuth, Tellurium, Cadmium, Zinc, and Tin scheme, *Proceedings of the American Academy of Arts and Sciences* 60(6): 305–383

Cao B, Cai W, Li Y, Sun F, Zhang L (2005) Ultraviolet-light-emitting ZnO nanosheets prepared by a chemical bath deposition method. *Nanotechnology* 16(9): 1734

Chang SJ, Hsueh TJ, Hsueh HT, Hung FY, Tsai TY, Weng WY, Hsu CL, Dai BT (2011) CuO nanowire-based humidity sensors prepared on glass substrate. *Sensors and Actuators B Chemical* 156: 906-9

Chen JW, Perng DC, Fang JF (2011) Nano-structured Cu<sub>2</sub>O solar cells fabricated on sparse ZnO nanorods, solar energy mater, *Solar Cells* 95: 2471–2477

Czochralski J (1918) A new method for the measurement of the crystallization rate of metals. *Zeitschrift für physicalische chemie* 92: 219–221

Dimitriadis CA, Papadimitriou L, and NA (1983) Economou, Resistivity dependence of the minority carrier diffusion length in in single crystals of Cu<sub>2</sub>O. *Journal of Materials Science Letters* 2(11): 691-693

Dolui SK, Phukon P, Nath BC, Das D (2013) Synthesis and evaluation of antioxidant and antibacterial behavior of CuO nanoparticles. *Colloids and Surfaces B: Biointerfaces* 101: 430-433

Erdoğan İY, Demir U (2009) Synthesis and characterization of Sb<sub>2</sub>Te<sub>3</sub>nanofilms via electrochemical co-deposition method. *Journal of Electroanalytical Chemistry* 633: 253-258

Erdoğan İY, Oznuluer T, Bulbul F, Demir U (2009) Characterization of size-quantized PbTe thin films synthesized by an electrochemical co-deposition method. *Thin Solid Films* 517: 5419-5424

Erdoğan İY, Demir U (2010) One-step electrochemical preparation of the ternary (Bi<sub>x</sub>Sb<sub>1-x</sub>)<sub>2</sub>Te<sub>3</sub> thin films on Au(111), Composition-dependent growth and characterization studies. *ElectrochimicaActa* 55: 6402-6407

Erdoğan İY, Demir U (2011) Orientation-controlled synthesis and characterization of Bi<sub>2</sub>Te<sub>3</sub>nanofilms and nanowires via electrochemical co-deposition. *ElectrochimicaActa* 56: 2385-2393

Feng X, Guo C, Mao L, Ning J, Hu Y (2014) Facile growth of Cu<sub>2</sub>O nanowires on reduced graphene sheets with high nonenzymatic electrocatalytic activity toward glucose. *Journal of the American Ceramic Society* 97(3): 811-815

Fernando CAN, Wethasinghe SK (2000) Investigation of Photoelectrochemical Characteristics of n-Type Cu<sub>2</sub>O Films. *Solar energy mater, Solar Cells* 63: 299–308

Fung KZ, Liao CL, Chang ST, Leu IC, Lee YH (2004) The electrochemical capacities and cycle retention of electrochemically deposited Cu<sub>2</sub>O thin film toward lithium. *Science direct* 50: 553-559

Gao F, Yu KM, Mendelsberg RJ, Anders A, Walukiewicz W (2011) Preparation of high transmittance ZnO Al film by pulsed filtered cathodic arc technology and rapid thermal annealing. *Applied surface science* 257(15): 7019-7022

Golden TD, Shumsky MG, Zhou Y, Vanderwerf RA, Vanleeuwen RA, witzer JA (1996) Electrochemical deposition of copper (I) oxide films. *Chemistry of materials* 8(10): 2499-2504

Goodridge F, King CJH (1974) *Technique of electroorganic synthesis. Part 1*, weinberg NL, Ed, wiley, NewYork

He S, Amoruso S, Pang D, Wang C, Hu M (2016) Chromatic annuli formation and sample oxidation on copper thin films by femtosecond laser. *The Journal of chemical physics* 144(16): 164703

Heyrovsky J (1922) Elektrolýsa se rtufovou kapkovou katódou. *Chem. Listy* 16: 256-264

Janotti A, Vandewalle CG (2009) Fundamentals of zinc oxide as a semiconductor. *Rep prog physic* 72(12): 126501

Jayathileke KMDC, Siripala W, Jayanettib JKDS (2008) Electrodeposition of p-type, n-type and p-n Homojunction Cuprous Oxide Thin Films. *Sri Lanka Journal of Physics* Volume 9: 35-46

Jayewardena C, Hewaparakrama KP, Wijewardena, DLA, Guruge H (1998) Fabrication of n-Cu<sub>2</sub>O Electrodes with Higher Energy Conversion Efficiency in a Photoelectrochemical Cell, *solar energy mater, solar cells* 56: 29–33

Jeong SH, Song SH, Nagaich K, Campbell SA, Aydil ES (2011) An analysis of temperature dependent current voltage characteristics of Cu<sub>2</sub>O-ZnO heterojunction solar cells. *Thin Solid Films* 519: 6613–9

Jiang T, Xie T, Yang W, Chen L, Fan H, Wang D (2013) Photoelectrochemical and Photovoltaic Properties of p-n Cu<sub>2</sub>O Homojunction Films and their Photocatalytic Performance. *Journal Physical Chemistry* 117: 4619–4624

Jiang X, Lin Q, Zhang M, He G, Sun, Z (2015) Microstructure, optical properties, and catalytic performance of Cu<sub>2</sub>O-modified ZnO nanorods prepared by electrodeposition. *Nanoscale Research Letters* 10(1): 2–7

Jonghde, PE, Vanmaekelbergh D, Kelly JJ (1999) Cu<sub>2</sub>O Electrodeposition and Characterization. *Chemistry Materials* 11: 3512– 3517

Kandjani AE, Sabri YM, Periasamy SR, Zohora N, Amin MH, Nafady A, Bhargava SK (2015) Controlling core/shell formation of nanocubic p-Cu<sub>2</sub>O/n-ZnO toward enhanced photocatalytic performance. *Langmuir* 31(39): 10922-10930

Khan R, Yun JH, Lee IH, Vaseem M, Hahn YB (2016) Improved optical transparency of CuO films prepared by using quantum-dot ink on glass substrates. *Journal of the Korean Physical Society* 68(1): 68-72

Kim J, Kim W, Yong K (2012) CuO/ZnO heterostructured nanorods photochemical synthesis and the mechanism of H<sub>2</sub>S gas sensing. *The Journal of Physical Chemistry* 116(29): 15682-15691

Klingshirn CF. (2010) Zinc Oxide from fundamental properties towards novel applications. Heidelberg, London/Springer; Klingshirn C, *Physical Status Solidi b* 71 547

Krishnan S, Ranganathan B (2013) Influence of K-doping on the optical properties of ZnO thin films grown by chemical bath deposition method. *Journal of Alloys and Compounds* 562: 187-193

Kroger FA, Panicker MPR, Knaster M (1978) Cathodic Deposition Of CdTe From Aqueous-Electrolytes. *Journal of the Electrochemical Society* 125: 566-572

Lee DS, Park KH, Park JW, Jung MY, Kang, H, Choi NJ, Park HJ (2014) A ppb level formaldehyde gas sensor based on CuO nanocubes prepared using a polyol process. *Sensors and Actuators B Chemical* 203: 282-288

Li F, Fan G (2011) Effect of sodium borohydride on growth process of controlled flowerlike nanostructured Cu<sub>2</sub>O/CuO films and their hydrophobic property. *Chemical Engineering Journal* 167: 388-396

Li J, Li H, Xue Y, Fang H, Wang W (2014) Facile electrodeposition of environment friendly Cu<sub>2</sub>O/ZnO heterojunction for robust photoelectrochemical biosensing. *Sensors and Actuators B Chemical* 191: 619-624

Lin JC, Huang MC, Wang TS, Chang WS, Wu CC, Chen C I, Peng KC, Lee SW (2014) Temperature dependence on p-Cu<sub>2</sub>O thin film electrochemically deposited onto copper substrate. *Applied Surface Science* 301: 369-377

Lin Y, Wei W, Wang Y, Zhou J, Sun D, Zhang X, Ruan S (2015) High stabilized and rapid sensing acetone sensor based on Au nanoparticle-decorated flower-like ZnO microstructures. *Journal of Alloys and Compounds* 650: 37-44

Liu X, Zhang J, Guo X, Wu S, Wang S (2010) Porous-Fe<sub>2</sub>O<sub>3</sub> decorated by Au nanoparticles and their enhanced sensor performance. *Nanotechnology* 21(9): 095501

Liu XW, Wang FY, Zhen F, Huang JR (2012) In situ growth of Au nanoparticles on the surfaces of Cu<sub>2</sub>O nanocubes for chemical sensors with enhanced performance. *RSC Advances* 2(20): 7647-7651

Lyu SC, Zhang Y, Lee CJ, Ruh H, Lee HJ (2003) Low-temperature growth of ZnO nanowire array by a simple physical vapor-deposition method. *Chemistry of materials* 15(17): 3294-3299

Ma Y, Li X, Yang Z, Xu S, Zhang W, Su Y, Zhang Y (2016) Morphology Control and Photocatalysis Enhancement by in Situ Hybridization of Cuprous Oxide with Nitrogen Doped Carbon, Quantum Dots. *Langmuir* 32(37): 9418-9427

Malachuk PA (1969) Correlation of linear sweep voltammetric and chronoamperometric data for n-value determinations. *Analytical Chemistry* 41: 1493



Malerba C, Biccari F, Ricardo ALC, Incau DM, Scardi P, Mittiga A (2011) Solar Energy Mater. Solar Cells 95: 2848

Mathew X, Mathews NR, Sebastian PJ (2011) Temperature dependence of the optical transitions in electrodeposited  $\text{Cu}_2\text{O}$  thin films. Solar Energy Materials and Solar Cells 70: 277-286

McShane CM, Choi KS (2009) Photocurrent Enhancement of n-Type  $\text{Cu}_2\text{O}$  Electrodes Achieved by Controlling Dendritic Branching Growth. Journal American Chemistry Society 131: 2561–2569

Mohd YS, Md I, Abubakar S, Hashim N, Ghani S (2014) A review of glucose biosensors based on graphene/metal oxide nanomaterials. Analytical letters 47(11): 1821-1834

Morkoç H, Özgür Ü (2009) General properties of Zinc Oxide  $\text{ZnO}$ . Fundamentals Materials and Device Technology 1-76

Mukherjee N, Mondal A, Khan GG, Mitra BC, Bhar SK, Madhu U, Maji SK, Show B (2011)  $\text{CuO}$  nano-whiskers, Electrodeposition, Raman analysis, photoluminescence study and photocatalytic activity. Materials Letters 65: 3248-3250

Nawar AM, Aal NA, Said N, El-Tantawy F, Yakuphanoglu F (2014) Improving the optical and electrical properties of Zinc Oxide thin film by Cupric Oxide dopant. IOSR Journal of Applied Physics (IOSR-JAP) e-ISSN: 2278-4861. Volume 6, Issue 4 Ver. II (Jul-Aug) PP 17-22

Noda S, Shima H, Akinaga H (2013)  $\text{Cu}_2\text{O}/\text{ZnO}$  hetero junction solar cells fabricated by magnetron sputter deposition method films using sintered ceramics targets. Journal Physical Conf. Ser 433: 012027-1–10

Nolan MSD, Elliott (2006) The p-type conduction mechanism in  $\text{Cu}_2\text{O}$ . a first principles study. Physical Chemical and Chemo Physics 8: 5350–5358

Okuyama K, Lenggoro W, Project N (2005) Nanoparticle Preparation and Its Application. A Nanotechnology Particle Project in Japan 1–4

Pan L, Zou JJ, Zhang T, Wang S, Li Z, Wang L, Zhang X (2013)  $\text{Cu}_2\text{O}$  film via hydrothermal redox approach: morphology and photocatalytic performance. The Journal of Physical Chemistry C 118(30): 16335-16343

Pan Y, Deng S, Polavarapu L, Gao N, Yuan P, Sow CH, Xu QH (2012) Plasmon-enhanced photocatalytic properties of  $\text{Cu}_2\text{O}$  nanowire-Au nanoparticle assemblies. Langmuir 28(33): 12304-12310

Pierson JF, Wang Y, Ghanbaja J, Soldera F, Boulet P, Horwat D, Mücklich F (2014) Controlling the preferred orientation in sputter-deposited Cu<sub>2</sub>O thin films, Influence of the initial growth stage and homoepitaxial growth mechanism. *Science Direct* 76: 207- 212

Reut G, Oksenberg E, Popovitz-biro R, Rechav K, Joselevich E (2016) Guided Growth of Horizontal p-Type ZnTe Nanowires 6b: 05191

RyuH, Kim TG, Oh H, Lee, WJ (2014) The study of post annealing effect on Cu<sub>2</sub>O thinfilms by electrochemical deposition for photoelectrochemical applications. *Journal of Alloys and Compounds* 612: 74-79

Sáenz A, Amézag P, Pizá P, Solís O, Ornelas C, Pérez S, Miki M (2014) Microstructural characterization, optical and photocatalytic properties of bilayered CuO and ZnO based thin films. *Journal of Alloys and Compounds* 615: S375-S381

Şahin ME, Okumuş HI (2016) Physical Structure, Electrical Design, Mathematical Modeling and Simulation of Solar Cells and Modules. *Turkish Journal of Electromechanics and Energy* Volume 1 Page: 1-8

Sathyamoorthy R, Mageshwari K (2013) Physical properties of nanocrystalline CuO thin films prepared with the SILAR method. *Materials Science in Semiconductor Processing* 16: 337-343

Sato M, Honda T, Takano I, Mochizuki C, Hara H, Suzuki T, Nagai H C (2012) hemical fabrication of p-type Cu<sub>2</sub>O transparent thin film using molecular precursor method. *Materials Chemistry and Physics* 137: 252-257

Scanlon DO, Watson GW (2011) Uncovering the complex behavior of hydrogen in Cu<sub>2</sub>O. *Physical*

Siripala W (2008) Electrodeposition of n-type Cuprous Oxide Thin Films. *ECS Transactions* 11 (9): 1-10

Skoog DA, Holler FJ, Nieman TA (1998) *Principles of Instrumental Analysis*, Edition Harbor Drive, part IV, Orlando, Florida

Solmaz R, Döner A, Doğrubaş M, Erdoğan İY, Kardaş G (2016) Enhancement of electrochemical activity of Raney-type NiZn coatings by modifying with PtRu binary deposits, Application for alkaline water electrolysis. *International Journal of Hydrogen Energy* 41(3): 1432-1440

Stadtländer CTKH (2007) Scanning electron microscopy and transmission electron microscopy of mollicutes: challenges and opportunities. *Modern research and educational topics in microscopy* 1: 122-131

Stoppato A (2008) Life cycle assessment of photovoltaic electricity generation *Energy* 33(2): 224-232

Sze SM, Ng KK (2007) *Physics of Semiconductor Devices*. John Wiley Sons, New York, 3rd editin

Tsui LK,Zangari G (2013) The Influence of Morphology of Electrodeposited  $\text{Cu}_2\text{O}$  and  $\text{Fe}_2\text{O}_3$  on the Conversion Efficiency of  $\text{TiO}_2$  Nanotube Photoelectrochemical Solar Cells. *Electrochim.Acta* 100: 220-225

URL-1, <http://www.bayar.edu.tr/besergil/eak-2-1-referans.pdf> (erişimtarihi: 23.05.2015)

URL-2, <abs.mehmetakif.edu.tr/upload/1127-904-dosya.pdf> (erişimtarihi: 22.05.2015)

URL-3, <http://www.uksaf.org/tech/edx.html> (erişimtarihi: 22.08.2016)

URL-4, <http://www.mri.psu.edu/mcl/techniques/eds.asp> (erişimtarihi: 22.08.2016)

Weinberg NL (1972) Simplified Construction of Electrochemical Cells. *Journal of Chemistry Education* 49: 120

Wijesundera RP, Hidaka M, Koga K, Sakai M,Siripala W, Choi JY, Sung NE (2007) Effects of Annealing on the Properties and Structure of Electrodeposited Semiconducting Cu-O Thin Films. *Phys. Status Solidi B*, 244: 4629-4642

Yamazoe N, Sakai G, Shimano K (2003) Oxide semiconductor gas sensors. *Catalytically Server Asia* 7: 63-75

Yang Y, Han J, Ning X, Cao W, Xu W, Guo L (2014) Controllable morphology and conductivity of electrodeposited  $\text{Cu}_2\text{O}$  thin film: effect of surfactants. *ACS applied materials interfaces* 6(24): 22534

Zhang J, Zhu H, Li C, Pan F, Wang T, Huang B (2009)  $\text{Cu}_2\text{O}$  thin films deposited by reactive direct current magnetron sputtering. *Thin Solid Films* 517: 5700-5704

ZhangL, McMillon L, McNatt J (2013) Gas-dependent bandgap and electrical conductivity of  $\text{Cu}_2\text{O}$  thin films. *Solar Energy Materials, Solar Cells* 108: 230-234

Zhang W, Yang X, Zhu Q, Wang K, Lu J, Chen M, Yang Z (2014) One-pot room temperature synthesis of  $\text{Cu}_2\text{O}/\text{Ag}$  composite nanospheres with enhanced visible-light-driven photocatalytic performance. *Industrial & Engineering Chemistry Research* 53(42): 16316-16323

Zhao W, Fu W, Yang H, Tian C, Li M, Li Y, Zhang L, Sui Y, Zhou X, Chen H, Zou G (2011) Electrodeposition of Cu<sub>2</sub>O Films and Their Photoelectrochemical Properties. *Crystal Engineering Common* 13: 2871–2877

Zhu W, Liu X, Liu H, Tong D, Yang J, Peng J (2010) Coaxial heterogeneous structure of TiO<sub>2</sub> nanotube arrays with CdS as a superthin coating synthesized via modified electrochemical atomic layer deposition. *Journal of the American Chemical Society* 132(36): 12619-12626

## **CURRICULUM VITAE**

In 1985, I had born in Kanispika village/Shahrazoor /Sulaimani. I completed primary and secondary school in sulaimani. And then, In 2009-2010, I graduated in Sulaimani University/college of science/chemical department, successfully. In addition, after four years, I hold the bachelors certification in that field, approximately, one year after of my graduation, I started to the work as the assistance of chemistry in the Technical college of Agriculture in Halabja / Sulaimani Polytechnic University of Iraq. Furthermore, In February of 2015, I started to the study of my master degree in Bingöl University/Institute of Science and Technology/ Turkey. Chemistry Department/Analytical chemistry.

**AKO MAHMOOD QADIR**

Email: shalaw.mahmud86@gmail.com

Asia cell: +9647701515697

Korektel: +9647501171511